Geochemistry of the dissolved loads during high-flow season of rivers in Southeast Coastal Region, China: Anthropogenic impact on chemical weathering and carbon sequestration

Wenjing Liu[1,2,3], Zhifang Xu[1,2,3*], Huiguo Sun[1,3], Tong Zhao[1,3], Chao Shi[3], Taoze Liu[4]

[1] Key Laboratory of Cenozoic Geology and Environment, Institute of Geology and Geophysics, Institutions of Earth Science, Chinese Academy of Sciences, Beijing 100029, China

[2] CAS Center for Excellence in Life and Paleoenvironment, Beijing, 100044, China

[3] University of Chinese Academy of Sciences, Beijing 100049, China

[4] State Key Laboratory of Environmental Geochemistry, Institute of Geochemistry, Chinese Academy of Sciences, Guiyang, Guizhou 550002, China

* Corresponding author. zfxu@mail.iggcas.ac.cn (Zhifang Xu, Tel: +86 10 82998289)

Abstract:

Southeast coastal region is one of the most developed and populated area in China. Meanwhile, it has been a severe acid rain impacted region for many years. The chemical compositions and carbon isotope composition of dissolved inorganic carbon ($\delta^{13}C_{DIC}$) of river waters in high flow season were investigated to estimate the chemical weathering and associated atmospheric CO_2 consumption rates, as well as the acid deposition disturbance on them. Mass balance calculation indicated that the dissolved loads of major rivers in the Southeast Coastal Rivers Basin (SECRB) were contributed by atmospheric (14.3%, 6.6-23.4%), anthropogenic (15.7%, 0-41.1%), silicate weathering (39.5%, 17.8-74.0%) and carbonate weathering inputs (30.6%, 3.9-62.0%). The silicate and carbonate chemical weathering rates for these river watersheds were 14.2-35.8 t km^{-2} a^{-1} and 1.8-52.1 t km^{-2} a^{-1}, respectively. The associated mean CO_2 consumption rate by silicate weathering for the whole SECRB were 191×10^3 mol km^{-2} a^{-1}. The chemical and $\delta^{13}C_{DIC}$ evidences indicated that sulfuric and nitric acid (mainly from acid deposition) was significantly involved in chemical weathering of rocks. There was an overestimation of CO_2 consumption at 0.19×10^{12} g C a^{-1} if sulfuric and nitric acid was ignored, which accounted for about 33.6% of the total CO_2 consumption by silicate weathering in the SECRB. This study quantitatively highlights the role of acid deposition in chemical weathering, suggesting that anthropogenic impact should be seriously considered in estimation of chemical weathering and associated CO_2 consumption.

1. Introduction

Chemical weathering of rocks is the key process that links geochemical cycling of solid earth to the atmosphere and ocean. It provides nutrients to terrestrial and marine ecosystems and regulates the level of atmospheric CO_2. As a net sink of atmospheric CO_2 on geologic timescales, estimation of silicate chemical weathering rates and the controlling factors are important issues related to long-term global climate change (e.g. Raymo and Ruddiman, 1992; Négrel et al. 1993; Berner and Caldeira, 1997; Gaillardet et al., 1999; Kump et al., 2000; Amiotte-Suchet et al., 2003; Oliva et al., 2003; Hartmann et al., 2009; Moon et al., 2014). As an important component in the Earth's Critical Zone (U.S. Nat. Res. Council Comm., 2001), river serves as an integrator of various natural and anthropogenic processes and products in a basin, and a carrier transporting the weathering products from continent to ocean. Therefore, the chemical compositions of river waters are widely used to evaluate chemical weathering and associated CO_2 consumption rates at catchment and/or continental scale, and to examine their controlling factors (e.g., Edmond et al., 1995; Gislason et al., 1996; Galy and France-Lanord, 1999; Huh, 2003; Millot et al., 2002, 2003; Oliva et al., 2003; West et al., 2005; Moon et al., 2007; Noh et al., 2009; Shin et al., 2011; Calmels et al., 2011; Li, S., et al. 2014).

With the intensification of human activities, human perturbations to river basins have increased in frequency and magnitude (Raymond et al., 2008; Regnier et al., 2013; Li and Bush, 2015). It is important to understand how such perturbations function on the current weathering systems and to predict how they will affect the Critical Zone of

56 the future (Brantley and Lebedeva, 2011). In addition to CO_2, other sources of acidity
57 (such as sulfuric, nitric and organic acids) can also produce protons. These protons react
58 with carbonate and silicate minerals, thus enhance rock chemical weathering rate and
59 flux compared with only considering protons deriving from CO_2 dissolution (Calmels
60 et al., 2007; Xu and Liu, 2010). The effect of other sourced proton (especially H^+
61 induced by SO_2 and NO_X coming from anthropogenic activities) on chemical
62 weathering is documented to be an important mechanism modifying atmospheric CO_2
63 consumption by rock weathering (Galy and France-Lanord, 1999; Semhi, et al., 2000;
64 Spence and Telmer, 2005; Xu and Liu, 2007; Perrin et al., 2008; Gandois et al., 2011).
65 Anthropogenic emissions of SO_2 was projected to provide 3 to 5 times greater H_2SO_4
66 to the continental surface than the pyrite oxidation originated H_2SO_4 (Lerman et al.,
67 2007). Therefore, increasing acid precipitation due to intense human activities
68 nowadays could make this mechanism more prominently.

69 The role of acid precipitation plays on the chemical weathering and CO_2
70 consumption has been investigated in some river catchments (Amiotte-Suchet et al.,
71 1995; Probst et al., 2000; Vries et al., 2003; Lerman et al., 2007; Xu and Liu, 2010). It
72 has been documented that silicate rocks were more easily disturbed by acid
73 precipitation during their weathering and soil leaching processes, because of their low
74 buffeting capacity (Reuss et al., 1987; Amiotte-Suchet et al., 1995). The disturbance
75 could be intensive and cause a decrease of CO_2 consumption by weathering at about
76 73% due to acid precipitation in the Strengbach catchment (Vosges Mountains, France),
77 which is dominated by crystalline rocks (Amiotte-Suchet et al., 1995). This highlights

78 the importance of exploring anthropogenic impact on chemical weathering and CO_2
79 consumption under different background (e.g. lithology, climate, human activity
80 intensity, and basin scale) for better constraining and estimation of acid precipitation
81 effect on rock weathering. Asia, especially East Asia, is one of the world's major sulfur
82 and nitrogen emission areas. However, the effect of acid precipitation on silicate
83 weathering and associated CO_2 consumption has not been well evaluated in this area,
84 especially lacks quantitative studies.

85 Acid precipitation affected about 30% of the territory of China (Fig. 1), and the
86 seriously polluted areas are mainly located in the east, the south and the center of China,
87 where over 70% of the cities were suffering from acid rain (Zhang et al., 2007a; State
88 Environmental Protection Administration of China, 2009). Southeast coastal region of
89 China is one of the most developed and populated areas of this country, dominated by
90 Mesozoic magmatic rocks (mainly granite and volcanic rocks) in lithology. Meanwhile,
91 the southeast coastal area has become one of the three major acid rain areas in China
92 since the beginning of 1990s (Larssen et al., 1999). It is seriously impacted by acid rain,
93 with a volume-weighted mean value of pH lower than 4.5 for many years (Wang et al.,
94 2000; Larssen and Carmichael, 2000; Zhao, 2004; Han et al., 2006; Larssen et al., 2006;
95 Zhang et al., 2007a; Huang et al., 2008; Xu et al., 2011). Therefore, it is an ideal area
96 for evaluating silicate weathering and the associated acid rain effects. In the previous
97 work, we have recognized and discussed the importance of sulfuric acid on the rock
98 weathering and associated CO_2 consumption in the Qiantang river basin in this area
99 (Liu et al., 2016). However, it is difficult to infer the anthropogenic impact on chemical

100 weathering and CO_2 consumption in the whole southeast coastal area from the case
101 study of a single river basin, because of the variations on lithology, basin scale, runoff
102 and anthropogenic condition in the large acid deposition affected area. In this study, the
103 chemical and carbon isotope composition of river waters in this area were first
104 systematically investigated, in order to: (i) decipher the different sources of solutes and
105 to quantify their contributions to the dissolved loads; (ii) calculate silicate weathering
106 and associated CO_2 consumption rates; (iii) evaluate the effects of acid deposition on
107 rock weathering and CO_2 consumption flux in the whole southeast coastal river basins.

108 **2. Natural setting of study area**

109 Southeast coastal region of China, where the landscape is dominated by
110 mountainous and hilly terrain, lacks the conditions for developing large rivers. The
111 rivers in this region are dominantly small and medium-size drainage due to the
112 topographic limitation. Only 5 rivers in this region have length over 200 km and the
113 drainage area over 10,000 km^2, and they are: the Qiantangjiang (Qiantang) and the
114 Oujiang (Ou) in Zhejiang province, the Minjiang (Min) and the Jiulongjiang (Jiulong)
115 in Fujian province and the Hanjiang (Han) in Guangdong province from north to south
116 (Fig. 1). Rivers in this region generally flow eastward or southward and finally inject
117 into the East China Sea or the South China Sea (Fig. 1), and they are collectively named
118 as 'Southeast Coastal Rivers' (SECRs).

119 The Southeast Coastal Rivers Basin (SECRB) is in the warm and humid
120 subtropical oceanic monsoon climate. The mean annual temperature and precipitation
121 are 17-21℃ and 1400-2000 mm, respectively. The precipitation mainly happens during

May to September, and the lowest and highest temperature often occurs in January and July. This area is one of the most developed areas in China, with a population more than 190 million (mean density of ~470 individuals/km^2), but the population mainly concentrated in the coastal urban areas. The vegetation coverage of these river basins is higher than 60%, mainly subtropical evergreen-deciduous broadleaf forest and mostly distributing in mountains area. Cultivated land, and industries and cities are mainly located in the plain areas and lower reach of these rivers.

Geologically, three regional-scale fault zones are distributed across the SECRB region (Fig. 1). They are the sub-EW-trending Shaoxing-Jiangshan fault zone, the NE-trending Zhenghe-Dapu fault zone, and the NE-trending Changle-Nanao fault zone (Shu et al., 2009). These fault zones dominate the direction of the mountains ridgelines and drainages, as well as the formation of the basins and bay. The Zhenghe-Dapu fault zone is a boundary line of Caledonian uplift belt and Hercynian-Indosinian depression zone. Mesozoic magmatic rocks are widespread in the southeast coastal region with a total outcrop area at about 240,000 km^2. Over 90% of the Mesozoic magmatic rocks are granitoids (granites and rhyolites) and their volcanic counterpart with minor existence of basalts (Zhou et al., 2000, 2006; Bai et al., 2014). These crust-derived granitic rocks are mainly formed in the Yanshanian stage, and may have been related to multiple collision events between Cathaysia and Yangtze blocks and Pacific plate (Zhou and Li, 2000; Xu et al., 2016). Among the major river basins, the proportions of magmatic rocks outcrop are about 36% in the Qiantang catchment, over 80% in the Ou, the Jiaoxi and the Jin catchments, and around 60% in the Min, the Jiulong, the Han and

144 the Rong catchments (Shi, 2014). The overlying Quaternary sediment in this area is
145 composed of brown-yellow siltstones but is rarely developed. The oldest basement
146 complex is composed of metamorphic rocks of greenschist and amphibolite facies.
147 Sedimentary rocks categories into two types, one is mainly composed by red clastic
148 rocks which cover more than 40,000 km^2 in the area; the other occurs as interlayers
149 within volcanic formations, including varicolored mudstones and sandstones. They are
150 mainly distributed on the west of Zhenghe-Dapu fault zone (FJBGRM, 1985; ZJBGMR,
151 1989; Shu et al., 2009).

152 **3. Sampling and analytical method**

153 A total of 121 water samples were collected from mainstream and tributaries of
154 the major rivers in the SECRB in July of 2010 in the high-flow period (sample number
155 and locations are shown in Fig. 1). For the river low reach samples, the sampling sites
156 were selected as far as possible from the tidal impacted area and the sampling were
157 conducted during low tide period (based on the daily tidal time,
158 http://ocean.cnss.com.cn/) in the sampling day. Besides, the salinity of the waters was
159 checked by salinometer (WS202, China) before sampling in the field. In addition, water
160 chemistry data were double checked to make sure that the river samples were not
161 contaminated by seawater. Water samples were collected in the middle channel of the
162 rivers from bridges or ferries, or directly from the center of some shallow streams.
163 Temperature (T), pH and electrical conductivity (EC) were measured in the field with
164 a portable EC/pH meter (YSI-6920, USA). All of the water samples for chemical
165 analysis were filtered in field through 0.22 μm Millipore membrane filter, and the first

166 portion of the filtration was discarded to wash the membrane and filter. One portion
167 filtrate was stored directly in HDPE bottles for anion analysis and another were
168 acidified to pH < 2 with 6 M double sub-boiling distilled HNO_3 for cation analysis. All
169 containers were previously washed with high-purity HCl and rinsed with Milli-Q 18.2
170 MΩ water.

171 Alkalinity was determined by phenolphthalein and methyl orange end point titration with
172 dilute HCl within 12 h after sampling. The HCl consumption volumes for phenolphthalein
173 and methyl orange end point titration were used to calculate the HCO_3^-. Cations (Na^+, K^+,
174 Ca^{2+} and Mg^{2+}) were determined using Inductively Coupled Plasma Atomic Emission
175 Spectrometer (ICP-AES) (IRIS Intrepid II XSP, USA). Anions (Cl^-, F^-, NO_3^- and SO_4^{2-})
176 were analyzed by ionic chromatography (IC) (Dionex Corporation, USA). Dissolved
177 silica was determined by spectrophotometry with the molybdate blue method. Reagent
178 and procedural blanks were measured in parallel to the sample treatment, and
179 calibration curve was evaluated by quality control standards before, during and after
180 the analyses of each batch of samples. Measurement reproducibility was determined by
181 duplicated sample and standards, which showed ±3% precision for the cations and ±5%
182 for the anions. Water chemistry analyzing was conducted in Hydrochemistry and
183 environmental laboratory, Institute of Geology and Geophysics, Chinese Academy of
184 Sciences.

185 Samples for carbon isotopic ratio ($\delta^{13}C$) of dissolved inorganic carbon (DIC)
186 measurements were collected in 150 ml glass bottles with air-tight caps and preserved
187 with $HgCl_2$ to prevent biological activity. The samples were kept refrigerated until

analysis. For the $\delta^{13}C$ measurements, the filtered samples were injected into glass bottles with phosphoric acid. The CO_2 was then extracted and cryogenically purified using a high vacuum line. $\delta^{13}C$ isotopic ratios were analyzed on Finnigen MAT-252 stable isotope mass spectrometer at the State Key Laboratory of Environmental Geochemistry, Chinese Academy of Sciences. The results are expressed with reference to VPDB, as follows:

$$\delta^{13}C = [(({}^{13}C/{}^{12}C)_{sample} / ({}^{13}C/{}^{12}C)_{standard}) - 1] \times 1000 \quad (1)$$

The $\delta^{13}C$ measurement has a precision of 0.1‰. A number of duplicate samples were measured, and the results show that the differences were less than the range of measurement accuracy.

4. Results

The major parameter and ion concentrations of samples are given in Table 1. The pH values of water samples ranged from 6.50 to 8.24, with an average of 7.23. Total dissolved solids (TDS) of water samples varied from 35.3 to 205 mg l^{-1}, with an average of 75.2 mg l^{-1}. Compared with the major rivers in China, the average TDS was significantly lower than the Changjiang (224 mg l^{-1}, Chetelat et al., 2008), the Huanghe (557 mg l^{-1}, Fan et al., 2014) and the Zhujiang (190 mg l^{-1}, Zhang et al., 2007b). However, the average TDS was comparable to the rivers draining silicate rock dominated areas, e.g. the upper Ganjiang in Ganzhou, south China (63 mg l^{-1}, Ji and Jiang, 2012), the Amur in north China (70 mg l^{-1}, Moon et al., 2009), the Xishui in Hubei, central China (101 mg l^{-1}, Wu et al., 2013), and north Han river in South Korea (75.5 mg l^{-1}, Ryu et al., 2008). Among the major rivers in the SECRB, the Qiantang had

the highest TDS value (averaging at 121 mg l^{-1}), and the Ou had the lowest TDS value (averaging at 48.8 mg l^{-1}).

Major ion compositions are shown in the cation and anion ternary diagrams (Fig. 2a and b). In comparison with rivers (e.g. the Wujiang and Xijiang) draining carbonate rocks dominated area (Han and Liu, 2004; Xu and Liu, 2010), these rivers in the SECRB had distinctly higher proportions of Na^+, K^+, and dissolved SiO_2. As shown in the Fig. 2, most samples had high Na^+ and K^+ proportions, with an average more than 50% (in μmol l^{-1}) of the total cations, except for samples from the Qiantang. The concentrations of Na^+ and K^+ ranged from 43.5 to 555 μmol l^{-1} and 42.9 to 233 μmol l^{-1}, with average values of 152 and 98 μmol l^{-1}, respectively. The concentrations of dissolved SiO_2 ranged from 98.5 to 370 μmol l^{-1}, with an average of 212 μmol l^{-1}. Ca^{2+} and Mg^{2+} accounted for about 38% and 11.6% of the total cation concentrations. HCO_3^- was the dominant anion with concentrations ranging from 139 to 1822 μmol l^{-1}. On average, it comprised 60.6% (36-84.6%) of total anions on a molar unit basis, followed by SO_4^{2-} (14.6%), Cl^- (13.1%) and NO_3^- (11.8%). The major ionic compositions indicate that water chemistry of these rivers in the SECRB is controlled by silicate weathering. Meanwhile, it is also influenced by carbonate weathering, especially for the Qiantang catchment.

The $\delta^{13}C$ of dissolved inorganic carbon in the rivers of the SECRB are also given in Table 1. The $\delta^{13}C$ of the water samples showed a wide range, from -11.0‰ to -24.3‰ (averaging at -19.4‰), and with a majority of samples falling into the range of -15 to -23‰. The values are comparable to rivers draining Deccan Traps (Das et al., 2005).

5. Discussion

232 The dissolved solids in river water are commonly from atmospheric and
233 anthropogenic inputs and weathering of rocks within the drainage basin. It is necessary
234 to quantify the contribution of different sources to the dissolved loads before deriving
235 chemical weathering rates and associated CO_2 consumption.

236 *5.1 Atmospheric and anthropogenic inputs*

237 To evaluate atmospheric inputs to river waters, chloride is the most common used
238 reference. Generally, water samples that have the lowest Cl^- concentrations are
239 employed to correct the proportion of atmospheric inputs in a river system (Négrel et
240 al., 1993; Gaillardet et al., 1997; Viers et al., 2001; Xu and Liu, 2007). In pristine areas,
241 the concentration of Cl^- in river water is assumed to be entirely derived from the
242 atmosphere, provided that the contribution of evaporites is negligible (e.g. Stallard and
243 Edmond, 1981; Négrel et al., 1993). In the SECRB, the lowest Cl^- concentration was
244 mainly found in the headwater of each river. According to the geologic setting, no salt-
245 bearing rocks was found in these headwater area (FJBGRM, 1985; ZJBGMR, 1989). In
246 addition, these areas are mainly mountainous and sparsely populated. Therefore, we
247 assumed that the lowest Cl^- concentration of samples from the headwater of each major
248 river came entirely from atmosphere.

249 The proportion of atmosphere-derived ions in the river waters can then be
250 calculated by the element/Cl ratios of the rain. Chemical compositions of rain in the
251 studied area have been reported at different sites, including Hangzhou, Jinhua, Nanping,
252 Fuzhou and Xiamen (Zhao, 2004; Zhang et al., 2007a; Huang et al., 2008; Cheng et al.,
253 2011; Xu et al., 2011) (Fig. 1). The volume-weighted mean concentration of ions and

Cl-normalized molar ratios are compiled in Table 2. Based on this procedure, 6.6-23.4% (averaging 14.3%) of total dissolved cations in the major rivers of the SECRB originated from rain. Among the anions, SO_4^{2-} and NO_3^- in the rivers are mainly from the atmospheric input, averaging at 73.2% for SO_4^{2-} and 75.8% for NO_3^-, respectively.

As one of the most developed and populated areas in China, the chemistry of river waters in the SECRB could be significantly impacted by anthropogenic inputs. Cl^-, NO_3^- and SO_4^{2-} are commonly associated with anthropogenic sources and have been used as tracers of anthropogenic inputs in watershed. High concentrations of Cl^-, NO_3^- and SO_4^{2-} can be found at the lower reaches of rivers in the SECRB, and there is an obvious increase after flowing through plain areas and cities. This tendency indicates that river water chemistry is affected by anthropogenic inputs while passing through the catchments. After correcting for the atmospheric contribution to river waters, the following assumption is needed to quantitatively estimate the contributions of anthropogenic inputs, which is that Cl^- originates from only atmospheric and anthropogenic inputs, and the excess of atmospheric Cl^- is regarded to present anthropogenic inputs and balanced by Na^+.

5.2 Chemical weathering inputs

Water samples were plotted on a plot of Na-normalized molar ratios (Fig. 3). The values of the world's large rivers (Gaillardet et al., 1999) are also shown in the figure. The best correlations between elemental ratios were observed for Ca^{2+}/Na^+ vs. Mg^{2+}/Na^+ ($R^2 = 0.95$, $n = 120$) and Ca^{2+}/Na^+ vs. HCO_3^-/Na^+ ($R^2 = 0.98$, $n = 120$). The samples cluster on a mixing line mainly between silicate and carbonate end-members,

276 closer to the silicate end-member, and showing little evaporite contribution. This
277 corresponds with the rock type distributions in the SECRB. In addition, all water
278 samples have equivalent ratios of $(Na^+ + K^+)/Cl^-$ larger than one, indicating silicate
279 weathering as the source of Na^+ and K^+ rather than chloride evaporites dissolution.
280 The geochemical characteristics of the silicate and carbonate end-members can be
281 deduced from the correlations between elemental ratios and referred to literature data
282 for catchments with well-constrained lithology. After correction for atmospheric inputs,
283 the Ca^{2+}/Na^+, Mg^{2+}/Na^+ and HCO_3^-/Na^+ of the river samples ranged from 0.31 to 30,
284 0.16 to 6.7, and 1.1 to 64.2, respectively. According to the geological setting (Fig. 1),
285 there are some small rivers draining purely silicate areas in the SECRs drainage basins.
286 Based on the elemental ratios of these rivers, we assigned the silicate end-member for
287 this study as $Ca^{2+}/Na^+=0.41\pm0.10$, $Mg^{2+}/Na^+=0.20\pm0.03$ and $HCO_3^-/Na^+=1.7\pm0.6$. The
288 ratio of $(Ca^{2+}+Mg^{2+})/Na^+$ for silicate end-member was 0.61 ± 0.13, which is close to the
289 silicate end-member of world rivers ($(Ca^{2+}+Mg^{2+})/Na^+ = 0.59\pm0.17$, Gaillardet et al.,
290 1999). Moreover, previous researches have documented the chemical composition of
291 rivers, such as the Amur and the Songhuajiang in North China, the Xishui in the lower
292 reaches of the Changjiang, and major rivers in South Korea (Moon et al., 2009; Liu et
293 al., 2013; Wu et al., 2013; Ryu et al., 2008; Shin et al., 2011). These river basins have
294 similar lithological setting with the study area, we could further validate the
295 composition of silicate end-member with their results. Ca^{2+}/Na^+ and Mg^{2+}/Na^+ ratios of
296 silicate end-member were reported for the Amur (0.36 and 0.22), the Songhuajiang
297 (0.44 ± 0.23 and 0.16), the Xishui (0.6 ± 0.4 and 0.32 ± 0.18), the Han (0.55 and 0.21) and

six major rivers in South Korea (0.48 and 0.20) in the studies above, well bracketing our estimation for silicate end-member.

Whereas, some samples show high concentrations of Ca^{2+}, Mg^{2+} and HCO_3^-, indicating the contribution of carbonate weathering. The samples from the upper reaches (Sample 12 and 13) of the Qiantang fall close to the carbonate end-member documented for world's large rivers (Gaillardet et al., 1999). In the present study, Ca^{2+}/Na^+ ratio of 0.41±0.10 and Mg^{2+}/Na^+ ratio of 0.20±0.03 for silicate end-member are used to calculate the contribution of Ca^{2+} and Mg^{2+} from silicate weathering. Finally, residual Ca^{2+} and Mg^{2+} are apportioned to carbonate weathering origin.

5.3 Chemical weathering rate in the SECRBs

Based on the above assumption, a forward model is employed to quantify the relative contribution of the different sources to the rivers of the SECRB in this study. (e.g. Galy and France-Lanord, 1999; Moon et al., 2007; Xu and Liu, 2007; 2010; Liu et al., 2013). The calculated contributions of different reservoir to the total cationic loads for major rivers and their main tributaries in the SECRB are presented in Fig. 4. On average, the dissolved cationic loads of the rivers in the study area originate dominantly from silicate weathering, which accounts for 39.5% (17.8-74.0%) of the total cationic loads in molar unit. Carbonate weathering and anthropogenic inputs account for 30.6% (3.9-62.0%) and 15.7% (0-41.1%), respectively. Contributions from silicate weathering are high in the Ou (55.6%), the Huotong (54.5%), the Ao (48.3%) and the Min (48.3%) river catchments, which are dominated by granitic and volcanic bedrocks. In contrast, high contribution from carbonate weathering is observed in the

Qiantang (54.0%), the Jin (52.2%) and the Jiulong (44.8%) river catchments. The results manifest the lithology control on river solutes of drainage basin.

The chemical weathering rate of rocks is estimated by the mass budget, basin area and annual discharge (data from the Annual Hydrological Report P. R. China, 2010, Table 3), expressed in t km^{-2} a^{-1}. The silicate weathering rate (SWR) is calculated using major cationic concentrations from silicate weathering and assuming that all dissolved SiO_2 is derived from silicate weathering (Xu and Liu, 2010), as the equation below:

$$SWR = ([Na]_{sil} + [K]_{sil} + [Ca]_{sil} + [Mg]_{sil} + [SiO_2]_{riv}) \times discharge/area \quad (2)$$

The assumption about Si could lead to overestimation of the silicate weathering rate, as part of silica may come from dissolution of biogenic materials rather than the weathering of silicate minerals (Millot et al., 2003; Shin et al., 2011). Thus, the cationic silicate weathering rates (Cat_{sil}) were also calculated.

The carbonate weathering rate (CWR) is calculated based on the sum of Ca^{2+}, Mg^{2+} and HCO_3^- from carbonate weathering, with half of the HCO_3^- coming from carbonate weathering being derived from the atmosphere CO_2, as the equation below:

$$CWR = ([Ca]_{carb} + [Mg]_{carb} + 1/2[HCO_3]_{carb}) \times discharge/area \quad (3)$$

The chemical weathering rate and flux are calculated for major rivers and their main tributaries in the SECRB, and the results are shown in Table 3. Silicate and carbonate weathering fluxes of these rivers (SWF and CWF) range from 0.02 $\times 10^6$ t a^{-1} to 1.80×10^6 t a^{-1}, and from 0.004×10^6 t a^{-1} to 1.74×10^6 t a^{-1}, respectively. Among the rivers, the Min has the highest silicate weathering flux, and the Qiantang has the highest carbonate weathering flux. On the whole SECRB scale, 3.95×10^6 t a^{-1} and 4.09×10^6 t

342 a^{-1} of dissolved solids originating from silicate and carbonate weathering, respectively,
343 are transported into the East and South China Sea by rivers in this region. Compared
344 with the largest three river basins (the Changjiang, the Huanghe and the Xijiang) in
345 China, the flux of silicate weathering calculated for the SECRB is lower than the
346 Changjiang (9.5×10^6 t a^{-1}, Gaillardet et al. 1999), but higher than the Huanghe
347 (1.52×10^6 t a^{-1}, Fan et al., 2014) and the Xijiang (2.62×10^6 t a^{-1}, Xu and Liu, 2010).
348 The silicate and carbonate chemical weathering rates for these river watersheds
349 were 14.2-35.8 t km^{-2} a^{-1} and 1.8-52.1 t km^{-2} a^{-1}, respectively. The total rock weathering
350 rate (TWR) for the whole SECRB is 48.1 t km^{-2} a^{-1}, higher than the world average (24
351 t km^{-2} a^{-1}, Gaillardet et al., 1999). The cationic silicate weathering rates (Cat_{sil}) ranges
352 from 4.7 to 12.0 t km^{-2} a^{-1} for the river watersheds in the SECRB, averaging at 7.8 t km^{-2} a^{-1}. Furthermore, a good linear correlation ($R^2 = 0.77$, n = 28) is observed between the
354 Cat_{sil} and runoff (Fig. 5), indicating that silicate weathering rates is controlled by runoff
355 as documented in previous researches (e.g., Bluth and Kump, 1994; Gaillardet et al.,
356 1999; Millot et al., 2002; Oliva et al., 2003; Wu et al., 2013; Pepin et al., 2013).

357 *5.4 CO_2 consumption and the role of sulfuric acid*

358 To calculate atmospheric CO_2 consumption by silicate weathering (CSW) and by
359 carbonate weathering (CCW), a charge-balanced state between rock chemical
360 weathering-derived alkalinity and cations was assumed (Roy et al., 1999).

361 $$[CO_2]_{CSW} = [HCO_3]_{CSW} = [Na]_{sil} + [K]_{sil} + 2[Ca]_{sil} + 2[Mg]_{sil} \quad (4)$$

362 $$[CO_2]_{CCW} = [HCO_3]_{CCW} = [Ca]_{carb} + [Mg]_{carb} \quad (5)$$

363 The calculated CO_2 consumption rates by chemical weathering for the rivers in

SECRB are shown in Table 3. CO_2 consumption rates by carbonate and silicate weathering are from 17.9 to 530×10^3 mol km^{-2} a^{-1} (averaging at 206×10^3 mol km^{-2} a^{-1}) and from 167 to 460×10^3 mol km^{-2} a^{-1} (averaging at 281×10^3 mol km^{-2} a^{-1}) for major river catchments in the SECRB. The CO_2 consumption rates by silicate weathering in the SECRB are higher than that of major rivers in the world and China, such as the Amazon (174×10^3 mol km^{-2} a^{-1}, Mortatti and Probst, 2003), the Mississippi and the Mackenzie (66.8 and 34.1×10^3 mol km^{-2} a^{-1}, Gaillardet et al., 1999), the Changjiang (112×10^3 mol km^{-2} a^{-1}, Chetelat et al., 2008), the Huanghe (35×10^3 mol km^{-2} a^{-1}, Fan et al., 2014), the Xijiang (154×10^3 mol km^{-2} a^{-1}, Xu and Liu, 2010), the Longchuanjiang (173×10^3 mol km^{-2} a^{-1}, Li et al., 2011) and the Mekong (191×10^3 mol km^{-2} a^{-1}, Li et al., 2014) and three large rivers in eastern Tibet (103-121×10^3 mol km^{-2} a^{-1}, Noh et al., 2009), the Hanjiang in central China (120×10^3 mol km^{-2} a^{-1}, Li et al., 2009) and the Sonhuajiang in north China (66.6×10^3 mol km^{-2} a^{-1}, Liu et al., 2013). The high CO_2 consumption rates by silicate weathering in the SECRB could be attributed to extensive distribution of silicate rocks, high runoff, favorable climatic conditions. The regional fluxes of CO_2 consumption by silicate and carbonate weathering is about 47.9×10^9 mol a^{-1} (0.57×10^{12} g C a^{-1}) and 41.9×10^9 mol a^{-1} (0.50×10^{12} g C a^{-1}) in the whole SECRB.

However, in addition to CO_2, the anthropogenic sourced proton (e.g. H_2SO_4 and HNO_3) is well documented as significant proton providers in rock weathering process (Galy and France-Lanord, 1999; Karim and Veizer, 2000; Yoshimura et al., 2001; Han and Liu, 2004; Spence and Telmer, 2005; Lerman and Wu, 2006; Xu and Liu 2007; 2010; Perrin et al., 2008; Gandois et al., 2011). Sulfuric acid can be generated by natural

386 oxidation of pyrite and anthropogenic emissions of SO_2 from coal combustion and
387 subsequently dissolve carbonate and silicate minerals. The riverine nitrate in a
388 watershed can be derived from atmospheric deposition, synthetic fertilizers, microbial
389 nitrification, sewage and manure, etc. (e.g. Kendall 1998). Although it is difficult to
390 determine the sources of nitrate in river waters, we can at least simply assume that
391 nitrate from acid deposition is one of the proton providers. The consumption of CO_2 by
392 rock weathering would be overestimated if H_2SO_4 and HNO_3 induced rock weathering
393 was ignored (Spence and Telmer, 2005; Xu and Liu, 2010; Shin et al., 2011; Gandois
394 et al., 2011). Thus, the role of the anthropogenic sourced protons plays on the chemical
395 weathering is crucial for an accurate estimation of CO_2 consumption by rock
396 weathering.

397 Rapid economic growth and increased energy needs have result in severe air
398 pollution problems in many areas of China, indicated by the high levels of mineral acids
399 (predominately sulfuric) observed in precipitation (Lassen and Carmichael, 2000; Pan
400 et al., 2013; Liu et al., 2016). The national SO_2 emissions in 2010 reached to 30.8
401 Tg/year (Lu et al., 2011). Previous study documented that fossil fuel combustion
402 accounts for the dominant sulfur deposition (~77%) in China (Liu et al., 2016). The wet
403 deposition rate of nitrogen is the highest in peaked over the central and south China,
404 with mean value of 20.2, 18.2 and 25.8 kg N ha^{-1} yr^{-1} in Zhejiang, Fujian and
405 Guangdong province, respectively (Lu and Tian, 2007). Current sulfur and nitrogen
406 depositions in the southeast coastal region are still among the highest in China (Fang et
407 al., 2013; Cui et al., 2014; Liu et al., 2016).

The involvement of protons originating from H_2SO_4 and HNO_3 in the river waters can be illustrated by the stoichiometry between cations and anions, shown in Fig. 6. In the rivers of the SECRB, the sum cations released by silicate and carbonate weathering could not be balanced by HCO_3^- only (Fig. 6a), but were almost balanced by the sum of HCO_3^-, SO_4^{2-} and NO_3^- (Fig. 6b). This implies that H_2CO_3, H_2SO_4 and HNO_3 are the potential erosion agents in chemical weathering in the SECRB. The $\delta^{13}C$ values of the water samples showed a wide range, from -11.0‰ to -24.3‰, with an average of -19.4‰. The $\delta^{13}C$ from soil is dominated by the relative contribution from C_3 and C_4 plant (Das et al., 2005). The studied areas have subtropical temperatures and humidity, and thus C_3 processes are dominant. The $\delta^{13}C$ of soil CO_2 is derived primarily from $\delta^{13}C$ of organic material which typically has value between -24 to -34‰, with an average of -28‰ (Faure, 1986). According to previous studies, the average value for C_3 trees and shrubs are from -24.4 to -30.5‰, and most of them are lower than -28‰ in south China (Chen et al., 2005; Xiang, 2006; Dou et al., 2013). After accounting for the isotopic effect from diffusion of CO_2 from soil, the resulted $\delta^{13}C$ (from the terrestrial C_3 plant process) should be ~ -25‰ (Cerling et al., 1991). This mean DIC derived from silicate weathering by carbonic acid (100% from soil CO_2) would yield a $\delta^{13}C$ value of -25‰. Carbonate rocks are generally derived from marine system and, typically, have $\delta^{13}C$ value close to zero (Das et al., 2005). Thus, the theoretical $\delta^{13}C$ value of DIC derived from carbonate weathering by carbonic acid (50% from soil CO_2 and 50% from carbonate rocks) is -12.5‰. DIC derived from carbonate weathering by sulfuric acid are all from carbonate rocks, thus the $\delta^{13}C$ of the DIC would be 0‰. Based on the above

discussion, sources of riverine DIC from different end-members in the SECRB were plotted in Fig. 7. Most water samples drift away from the three end-member mixing area (carbonate and silicate weathering by carbonic acid and carbonate weathering by sulfuric acid) and towards the silicate weathering by sulfuric and nitric acid area, clearly illustrating the effect of the anthropogenic sourced protons (sulfuric and nitric acid) on silicate weathering in the SECRB.

Considering the H_2SO_4 and HNO_3 effects on chemical weathering, CO_2 consumption by silicate weathering can be determined from the equation below (Moon et al., 2007; Ryu et al., 2008; Shin et al., 2011):

$$[CO_2]_{SNSW} = [Na]_{sil} + [K]_{sil} + 2[Ca]_{sil} + 2[Mg]_{sil} - \gamma \times [2SO_4 + NO_3]_{atmos} \quad (6)$$

Where γ is calculated by $cation_{sil}/(cation_{sil} + cation_{carb})$.

Based on the calculation in section 5.1, SO_4^{2-} and NO_3^- in river waters were mainly derived from atmospheric input. Assuming SO_4^{2-} and NO_3^- in river waters derived from atmospheric input (after correction for sea-salt contribution) are all from acid precipitation and considering H_2SO_4 and HNO_3 effects, CO_2 consumption rates by silicate weathering (SNSW) are estimated between 55×10^3 mol km^{-2} a^{-1} and 286×10^3 mol km^{-2} a^{-1} for major river watersheds in the SECRB. For the whole SECRB, the actual CO_2 consumption rates by silicate is 191×10^3 mol km^{-2} a^{-1} when the effect of H_2SO_4 and HNO_3 is considered. The flux of CO_2 consumption is overestimated by 16.1×10^9 mol a^{-1} (0.19×10^{12} g C a^{-1}) due to the involvement of H_2SO_4 and HNO_3 from acid precipitation, accounting for approximately 33.6% of total CO_2 consumption flux by silicate weathering in the SECRB. It highlights the fact that the drawdown of

atmospheric CO_2 by silicate weathering can be significantly overestimated if acid deposition is ignored in long-term perspectives. The result quantitatively shows that anthropogenic activities can significantly affect rock weathering and associated atmospheric CO_2 consumption. The quantification of this effect needs to be well evaluated in Asian and globally within the current and future human activity background.

It is noticeable that the chemical weathering and associated CO_2 consumption rates for the study area were calculated by the river water geochemistry of high-flow season. As a subtropical monsoon climate area, the river water of the southeast coastal rivers is mainly recharged by rain, and the amount of precipitation in high-flow season accounts for more than 70% of the annual precipitation in the area. The processes in low-flow season might be different for some extent. It is worth the further efforts to investigate the hydrology and temperature effect on weathering rate and flux, as well as on the anthropogenic impact evaluation in different climate regime and hydrology season.

6. Conclusions

River waters in the southeast coastal region of China are characterized by high proportions of Na^+, K^+ and dissolved SiO_2, indicating the water chemistry of the rivers in the SECRB is mainly controlled by silicate weathering. The dissolved cationic loads of the rivers in the study area originate dominantly from silicate weathering, which accounts for 39.5% (17.8-74.0%) of the total cationic loads. Carbonate weathering, atmospheric and anthropogenic inputs account for 30.6%, 14.3% and 15.7%, respectively. Meanwhile, more than 70% of SO_4^{2-} and NO_3^- in the river waters derived

from atmospheric input. The chemical weathering rate of silicates and carbonates for the whole SECRB are estimated to be approximately 23.7 and 24.5 t km^{-2} a^{-1}. About 8.04×10^6 t a^{-1} of dissolved solids originating from rock weathering are transported into the East and South China Sea by these rivers in the SECRB. With the assumption that all the protons involved in the weathering reaction are provided by carbonic acid, the CO_2 consumption rates by silicate and carbonate weathering are 287 and 251×10^3 mol km^{-2} a^{-1}, respectively. However, both water chemistry and carbon isotope data provide solid evidence that sulfuric and nitric acid from acid precipitation serves as significant agents during chemical weathering. Considering the effect of sulfuric and nitric acid, the CO_2 consumption rate by silicate weathering for the SECRB are 191×10^3 mol km^{-2} a^{-1}. Therefore, the CO_2 consumption flux would be overestimated by 16.1×10^9 mol a^{-1} (0.19×10^{12} g C a^{-1}) in the SECRB if the effect of sulfuric and nitric acid is ignored. This work quantitively illustrates that anthropogenic disturbance by acid precipitation has profound impact on CO_2 sequestration by rock weathering.

Acknowledgements. This work was financially supported by the Strategic Priority Research Program of Chinese Academy of Sciences，Grant No. XDB (Grant No. 26000000), and Natural Science Foundation of China (Grant No. 41673020, 91747202, 41772380 and 41730857).

References:

Amiotte-Suchet, P., Probst, A. Probst, J.-L., Influence of acid rain on CO_2 consumption by rock weathering: local and global scales. Water Air Soil Pollut. 85, 1563-1568, 1995.

496 Amiotte-Suchet, P., Probst, J.-L. Ludwig, W., Worldwide distribution of continental
497 rock lithology: implications for the atmospheric/soil CO_2 uptake by continental
498 weathering and alkalinity river transport to the oceans. Global Biogeochem.
499 Cycles 17, 1038-1052, 2003.
500 Bai, H., Song, L.S., Xia, W.P., Prospect analysis of hot dry rock (HDR) in Eastern part
501 of Jiangxi province, Coal Geol. China 26, 41-44. (In Chinese), 2014.
502 Berner, R.A., Caldeira, K., The need for mass balance and feedback in the geochemical
503 carbon cycle. Geology 25, 955-956, 1997.
504 Bluth, G.J.S., Kump, L.R., Lithological and climatological controls of river chemistry.
505 Geochim. Cosmochim. Acta 58, 2341-2359, 1994.
506 Brantley, S.L., Lebedeva, M., Learning to read the chemistry of regolith to understand
507 the Critical Zone. Annual Review of Earth and Planetary Sciences, 39: 387-416,
508 2011.
509 Calmels, D., Gaillardet, J., Brenot, A., France-Lanord, C., Sustained sulfide oxidation
510 by physical erosion processes in the Mackenzie River basin: climatic perspectives.
511 Geology 35, 1003-1006, 2007.
512 Calmels, D., Galy, A., Hovius, N., Bickle, M., West, A.J., Chen, M.-C., Chapman, H.,
513 Contribution of deep groundwater to the weathering budget in a rapidly eroding
514 mountain belt, Taiwan. Earth Planet. Sci. Lett. 303, 48-58, 2011.
515 Cerling, T.E., Solomon, D.K., Quade, J., Bownman, J.R., On the isotopic composition
516 of soil CO_2. Geochim. Cosmochim. Acta 55, 3403–3405, 1991.
517 Chen, Q., Shen, C., Sun, Y., Peng, S., Yi, W., Li Z., Jiang, M., Spatial and temporal

518 distribution of carbon isotopes in soil organic matter at the Dinghushan Biosphere
519 Reserve, South China. Plant and Soil, 273: 115–128, 2005.
520 Cheng, Y., Liu, Y., Huo, M., Sun, Q., Wang, H., Chen, Z., Bai, Y., Chemical
521 characteristics of precipitation at Nanping Mangdang Mountain in eastern China
522 during spring. J. Environ. Sci. 23, 1350-1358, 2011.
523 Chetelat, B., Liu, C., Zhao, Z., Wang, Q., Li, S., Li, J., Wang, B., Geochemistry of the
524 dissolved load of the Changjiang Basin rivers: anthropogenic impacts and
525 chemical weathering. Geochim. Cosmochim. Acta 72, 4254-4277, 2008.
526 Cui, J., Zhou, J., Peng, Y., He, Y., Yang, H., Mao, J., Atmospheric wet deposition of
527 nitrogen and sulfur to a typical red soil agroecosystem in Southeast China during
528 the ten-year monsoon seasons (2003-2012). Atmos. Environ. 82, 121-129, 2014.
529 Das, A., Krishnaswami, S., Sarin, M.M., Pande, K., Chemical weathering in the Krishna
530 Basin and Western Ghats of the Deccan Traps, India: Rates of basalt weathering
531 and their controls. Geochim. Cosmochim. Acta 69(8), 2067-2084, 2005.
532 Dou, X., Deng, Q., Li, M., Wang, W., Zhang, Q., Cheng, X., Reforestation of Pinus
533 massoniana alters soil organic carbon and nitrogen dynamics in eroded soil in
534 south China. Ecological Engineering 52, 154-160, 2013.
535 Edmond, J.M., Palmer, M.R., Measures, C.I., Grant, B., Stallard, R.F., The fluvial
536 geochemistry and denudation rate of the Guayana Shield in Venezuela, Colombia,
537 and Brazil. Geochim. Cosmochim. Acta 59, 3301-3325, 1995.
538 Fan, B.L, Zhao, Z.Q., Tao, F.X., Liu, B.J., Tao, Z.H., Gao, S., He, M.Y., Characteristics
539 of carbonate, evaporite and silicate weathering in Huanghe River basin: A

comparison among the upstream, midstream and downstream. J. Asian Earth Sci. 96, 17-26, 2014.

Fang, Y., Wang, X., Zhu, F., Wu, Z., Li, J., Zhong, L., Chen, D., Yoh, M., Three-decade changes in chemical composition of precipitation in Guangzhou city, southern China: has precipitation recovered from acidification following sulphur dioxide emission control? Tellus B 65, 1-15, 2013.

Faure, G., Principles of Isotope Geology. Wiley, Toronto, pp. 492-493, 1986.

FJBGMR: Fujian Bureau of Geology and Mineral Resources, Regional Geology of Fujian Province. Geol. Publ. House, Beijing, p. 671 (in Chinese with English abstract), 1985.

Gaillardet, J., Dupré, B., Allègre, C.J., Négrel, P., Chemical and physical denudation in the Amazon River basin. Chem. Geol. 142, 141-173, 1997.

Gaillardet, J., Dupré, B., Louvat, P., Allegre, C.J., Global silicate weathering and CO2 consumption rates deduced from the chemistry of large rivers. Chem. Geol. 159, 3-30, 1999.

Galy, A., France-Lanord, C., Weathering processes in the Ganges-Brahmaputra basin and the riverine alkalinity budget. Chem. Geol. 159, 31-60, 1999.

Gandois, L., Perrin, A.-S., Probst, A., Impact of nitrogenous fertilizer-induced proton release on cultivated soils with contrasting carbonate contents: A column experiment. Geochim. Cosmochim. Acta 75, 1185-1198, 2011.

Gislason, S.R., Arnorsson, S., Armannsson, H., Chemical weathering of basalt in southwest Iceland: effects of runoff, age of rocks and vegetative/glacial cover.

562 Am. J. Sci. 296, 837-907, 1996.
563 Han, G., Liu, C.Q., Water geochemistry controlled by carbonate dissolution: a study of
564 the river waters draining karst-dominated terrain, Guizhou Province, China.
565 Chem. Geol. 204, 1-21, 2004.
566 Han, Z.W., Ueda, H., Sakurai, T., Model study on acidifying wet deposition in East Asia
567 during wintertime. Atmos. Environ. 40, 2360-2373, 2006.
568 Hartmann, J., Jansen, N., Dürr, H.H., Kempe, S., Köhler, P., Global CO_2 consumption
569 by chemical weathering: what is the contribution of highly active weathering
570 regions? Global Planet. Change 69, 185-194, 2009.
571 Huang, K., Zhuang, G., Xu, C., Wang Y., Tang A., The chemistry of the severe acidic
572 precipitation in Shanghai, China. Atmos. Res. 89, 149-160, 2008.
573 Huh, Y.S., Chemical weathering and climate - a global experiment: a review. Geosci. J.
574 7, 277-288, 2003.
575 Hydrological data of river basins in Zhejiang, Fujian province and Taiwan region,
576 Annual Hydrological Report P. R. China, 2010, Vol (7) (in Chinese)
577 Ji, H., Jiang, Y., Carbon flux and C, S isotopic characteristics of river waters from a
578 karstic and a granitic terrain in the Yangtze River system. J. Asian Earth Sci. 57,
579 38-53, 2012.
580 Karim, A., Veizer, H.E., Weathering processes in the Indus River Basin: implication
581 from riverine carbon, sulphur, oxygen and strontium isotopes. Chem. Geol. 170,
582 153-177, 2000.
583 Kendall, C., Tracing nitrogen sources and cycling in catchments. In: Kendall, C., &

584 McDonnell, J.J., (Eds) Isotope Tracers in Catchment Hydrology. Elsevier,
585 Amsterdam, 1998.
586 Kump, L.R., Brantley, S.L., Arthur, M.A., Chemical weathering, atmospheric CO_2 and
587 climate. Ann. Rev. Earth Planet. Sci. 28, 611-667, 2000.
588 Larssen, T., Carmichael, G.R., Acid rain and acidification in China: the importance of
589 base cation deposition. Environ. Poll. 110, 89-102, 2000.
590 Larssen, T., Lydersen, E., Tang, D., He, Y., Gao, J., Liu, H., Duan, L., Seip, H.M., Acid
591 rain in China. Environ. Sci. Technol. 40, 418-425, 2006.
592 Lerman, A., Wu, L., CO_2 and sulfuric acid controls of weathering and river water
593 composition. J. Geochem. Explor. 88, 427-430, 2006.
594 Lerman, A., Wu, L., Mackenzie, F.T., CO_2 and H_2SO_4 consumption in weathering and
595 material transport to the ocean, and their role in the global carbon balance. Mar.
596 Chem. 106, 326-350, 2007.
597 Li, S., Bush, R.T., Changing fluxes of carbon and other solutes from the Mekong River.
598 Sci. Rep. 5, 16005, 2015.
599 Li, S.Y., Lu, X.X., Bush, R.T., Chemical weathering and CO_2 consumption in the Lower
600 Mekong River. Sci. Total Environ. 472, 162-177, 2014.
601 Li, S.Y., Lu, X.X., He, M., Zhou, Y., Bei, R., Li, L., Zieglera, A.D., Major element
602 chemistry in the Upper Yangtze River: a case study of the Longchuanjiang River.
603 Geomorphology129, 29-42, 2011.
604 Li, S.Y., Xu, Z.F., Wang, H., Wang, J.H., Zhang, Q.F., Geochemistry of the upper Han
605 River basin, China. 3: anthropogenic inputs and chemical weathering to the

606 dissolved load. Chem. Geol. 264, 89-95, 2009.
607 Liu, B., Liu, C.-Q., Zhang, G., Zhao, Z.-Q., Li, S.-L., Hu, J., Ding, H., Lang, Y.-C., Li.,
608 X.-D., Chemical weathering under mid- to cool temperate and monsoon-
609 controlled climate: A study on water geochemistry of the Songhuajiang River
610 system, northeast China. Appl. Geochem. 31, 265-278, 2013.
611 Liu, L., Zhang, X., Wang, S., Zhang, W., Lu, X., Bulk sulfur (S) deposition in China.
612 Atmos. Environ., 135, 41-49, 2016.
613 Liu, W., Shi, C., Xu, Z., Zhao, T., Jiang, H., Liang, C., Zhang, X., Zhou, Li., Yu, C.,
614 Water geochemistry of the Qiantangjiang River, East China: Chemical weathering
615 and CO_2 consumption in a basin affected by severe acid deposition. J.Asian Earth
616 Sci., 127, 246-256, 2016.
617 Lu, C., Tian, H., Spatial and temporal patterns of nitrogen deposition in China:
618 Synthesis of observational data. J. Geophys. Res. 112, D22S05, 2007.
619 Lu, Z., Zhang, Q., Streets, D.G., Sulfur dioxide and primary carbonaceous aerosol
620 emissions in China and India, 1996e2010. Atmos. Chem. Phys. 11, 9839-9864,
621 2011.
622 Millot, R., Gaillardet, J., Dupré, B., Allègre, C.J., Northern latitude chemical
623 weathering rates: clues from the Mackenzie River Basin, Canada. Geochim.
624 Cosmochim. Acta 67, 1305-1329, 2003.
625 Millot, R., Gaillardet, J., Dupré, B., Allègre, C.J., The global control of silicate
626 weathering rates and the coupling with physical erosion: new insights from rivers
627 of the Canadian Shield. Earth Planet. Sci. Lett. 196, 83-98, 2002.

628 Ministry of Environmental Protection of China, 2009. China Environmental Quality
629 Report 2008. China Environmental Sciences Press, Beijing. In Chinese.
630 Moon, S., Chamberlain, C.P., Hilley, G.E., New estimates of silicate weathering rates
631 and their uncertainties in global rivers. Geochim. Cosmochim. Acta 134, 257-274,
632 2014.
633 Moon, S., Huh, Y., Qin, J., van Pho, N., Chemical weathering in the Hong (Red) River
634 basin: Rates of silicate weathering and their controlling factors. Geochim.
635 Cosmochim. Acta 71, 1411-1430, 2007.
636 Moon, S., Huh, Y., Zaitsev, A., Hydrochemistry of the Amur River: Weathering in a
637 Northern Temperate Basin. Aquat. Geochem., 15, 497-527, 2009.
638 Mortatti, J., Probst, J.L., Silicate rock weathering and atmospheric/soil CO_2 uptake in
639 the Amazon basin estimated from river water geochemistry: seasonal and spatial
640 variations. Chem. Geol.197, 177-196, 2003.
641 Négrel, P., Allègre, C.J., Dupré, B., Lewin, E., Erosion sources determined by inversion
642 of major and trace element ratios and strontium isotopic ratios in river water: the
643 Congo Basin Case. Earth Planet. Sci. Lett. 120, 59-76, 1993.
644 Noh, H., Huh, Y., Qin, J., Ellis, A., Chemical weathering in the Three Rivers region of
645 Eastern Tibet. Geochim. Cosmochim. Acta 73, 1857-1877, 2009.
646 Oliva, P., Viers, J., Dupré B., Chemical weathering in granitic environments. Chem.
647 Geol. 202, 225-256, 2003.
648 Pan, Y.,Wang, Y., Tang, G., Wu, D., Spatial distribution and temporal variations of
649 atmospheric sulfur deposition in Northern China: insights into the potential

650 acidification risks. Atmos. Chem. Phys. 13, 1675-1688, 2013.
651 Pepin, E., Guyot, J.L., Armijos, E., Bazan, H., Fraizy, P., Moquet, J.S., Noriega, L.,
652 Lavado, W., Pombosa, R. Vauchel, P., Climatic control on eastern Andean
653 denudation rates (Central Cordillera from Ecuador to Bolivia). J. S. Am. Earth
654 Sci. 44, 85-93, 2013.
655 Perrin, A.-S., Probst, A., Probst, J.-L., Impact of nitrogenous fertilizers on carbonate
656 dissolution in small agricultural catchments: Implications for weathering CO_2
657 uptake at regional and global scales. Geochim, Cosmochim. Acta 72, 3105-3123,
658 2008.
659 Probst, A., Gh'mari, A.El., Aubert, D., Fritz, B., McNutt, R., Strontium as a tracer of
660 weathering processes in a silicate catchment polluted by acid atmospheric inputs,
661 Strengbach, France. Chem. Geol. 170, 203-219, 2000.
662 Raymo, M.E., Ruddiman,W.F., Tectonic forcing of late Cenozoic climate. Nature 359,
663 117-122, 1992.
664 Raymond, P. A., Oh, N.H., Turner, R.E., Broussard, W., Anthropogenically enhanced
665 fluxes of water and carbon from the Mississippi River. Nature 451, 449-452, 2008.
666 Regnier, P., Friedlingstein, P., Ciais, P., Mackenzie, F.T.,…Thullner. M., Anthropogenic
667 perturbation of the carbon fluxes from land to ocean. Nature Geosci. 6, 597-607.
668 2013.
669 Reuss, J.O., Cosby, B.J., Wright, RF., Chemical processes governing soil and water
670 acidification. Nature 329, 27-32, 1987.
671 Roy, S., Gaillardet, J., Allègre, C.J., Geochemistry of dissolved and suspended loads of

672 the Seine river, France: anthropogenic impact, carbonate and silicate weathering.
673 Geochim. Cosmochim. Acta 63, 1277-1292, 1999.
674 Ryu, J.S., Lee, K.S., Chang, H.W., Shin, H.S., Chemical weathering of carbonates and
675 silicates in the Han River basin, South Korea. Chem. Geol. 247, 66-80, 2008.
676 Semhi, K., Amiotte Suchet, P., Clauer, N., Probst, J.-L., Impact of nitrogen fertilizers
677 on the natural weathering-erosion processes and fluvial transport in the Garonne
678 basin. Appl. Geochem. 15 (6), 865-874, 2000.
679 Shi, C., Chemical characteristics and weathering of rivers in the Coast of Southeast
680 China (PhD Thesis). Institute of Geology and Geophysics, Chinese academy of
681 sciences, Beijing, China. pp, 1-100 (in Chinese with English abstract), 2014.
682 Shin, W.-J., Ryu, J.-S., Park, Y., Lee, K.-S., Chemical weathering and associated CO_2
683 consumption in six major river basins, South Korea. Geomorphology 129, 334-
684 341, 2011.
685 Shu, L.S., Zhou, X.M., Deng, P., Wang, B., Jiang, S.Y., Yu, J.H., Zhao, X.X., Mesozoic
686 tectonic evolution of the Southeast China Block: New insights from basin
687 analysis. J. Asian Earth Sci. 34(3), 376-391, 2009.
688 Spence, J., Telmer, K., The role of sulfur in chemical weathering and atmospheric CO_2
689 fluxes: Evidence from major ions, $\delta^{13}C_{DIC}$, and$\delta^{34}S_{SO4}$ in rivers of the Canadian
690 Cordillera. Geochim. Cosmochim. Acta 69, 5441-5458, 2005.
691 Stallard, R.F., Edmond, J.M., Geochemistry of the Amazon. Precipitation chemistry and
692 the marine contribution to the dissolved load at the time of peak discharge. J.
693 Geophys. Res., 86, 9844-9858, 1981.

694 U.S. Nat. Res. Council Comm., Basic Research Opportunities in Earth Science.
695 Washington, DC: Nat. Acad. 154 pp., 2001.
696 Viers, J., Dupré, B., Braun, J.J., Freydier, R., Greenberg, S., Ngoupayou, J.N.,
697 Nkamdjou, L.S., Evidence for non-conservative behavior of chlorine in humid
698 tropical environments. Aquat. Geochem. 7, 127-154, 2001.
699 Vries, W.D., Reinds, G.J. Vel E., Intensive monitoring of forest ecosystems in Europe.
700 2-Atmospheric deposition and its impacts on soil solution chemistry. For. Ecol.
701 Manage. 174, 97-115, 2003.
702 Wang, T.J., Jin, L.S., Li, Z.K., Lam K.S., A modeling study on acid rain and
703 recommended emission control strategies in China. Atmos. Environ. 34, 4467-
704 4477, 2000.
705 West, A.J., Galy, A., Bickle, M., Tectonic and climatic controls on silicate weathering.
706 Earth Planet. Sci. Lett. 235, 211-228, 2005.
707 Wu, W., Zheng, H., Yang, J., Luo, C., Zhou, B., Chemical weathering, atmospheric CO_2
708 consumption, and the controlling factors in a subtropical metamorphic-hosted
709 watershed. Chem. Geol. 356, 141-150, 2013.
710 Xiang, L., Study on Coupling between Water and Carbon of Artificial Forests
711 Communities in Subtropical Southern China. Master Dissertation, Institute of
712 Geographical Sciences and Natural Sources, Chinese Academy of Sciences,
713 China (in Chinese), 2006.
714 Xu, H., Bi, X-H., Feng, Y-C., Lin, F-M., Jiao, L., Hong, S-M., Liu, W-G., Zhang, X.-
715 Y., Chemical composition of precipitation and its sources in Hangzhou, China.

716 Environ. Monit. Assess. 183:581-592, 2011.
717 Xu, Y., Wang C.Y., Zhao T., Using detrital zircons from river sands to constrain major
718 tectono-thermal events of the Cathaysia Block, SE China. J. Asian Earth Sci. 124,
719 1-13, 2016.
720 Xu, Z., Liu, C.-Q., Chemical weathering in the upper reaches of Xijiang River draining
721 the Yunnan-Guizhou Plateau, Southwest China. Chem. Geol. 239, 83-95, 2007.
722 Xu, Z., Liu, C.-Q., Water geochemistry of the Xijiang basin rivers, South China:
723 Chemical weathering and CO_2 consumption. Appl. Geochem. 25, 1603-1614,
724 2010.
725 Yoshimura, K., Nakao, S., Noto, M., Inokura, Y., Urata, K., Chen, M., Lin, P.W.,
726 Geochemical and stable isotope studies on natural water in the Taroko Gorge karst
727 area, Taiwan - chemical weathering of carbonate rocks by deep source CO_2 and
728 sulfuric acid. Chem. Geol. 177, 415–430, 2001.
729 Zhang, M., Wang, S., Wu, F., Yuan, X., Zhang, Y., Chemical compositions of wet
730 precipitation and anthropogenic influences at a developing urban site in
731 southeastern China. Atmos. Res. 84, 311-322, 2007a.
732 Zhang, S.R., Lu, X. X., Higgitt, D. L., Chen, C.T.A., Sun, H.-G., Han, J.T., Water
733 chemistry of the Zhujiang (Pearl River): Natural processes and anthropogenic
734 influences. J. Geophys. Res. 112, F01011, 2007b.
735 Zhao, W., An analysis on the changing trend of acid rain and its causes in Fujian
736 Province. Fujian Geogr. 19, 1-5 (in Chinese), 2004.
737 Zhou, X.M., Li, W.X., Origin of Late Mesozoic igneous rocks in Southeastern China:

738 Implications for lithosphere subduction and underplating of mafic magmas.
739 Tectonophysics 326(3-4), 269-287, 2000.
740 Zhou, X.M., Sun, T., Shen, W.Z., et al., Petrogenesis of Mesozoic granitoids and
741 volcanic rocks in South China: A response to tectonic evolution. Episodes 29(1),
742 26-33, 2006.
743 ZJBGMR: Zhejiang Bureau of Geology and Mineral Resources, Regional Geology of
744 Zhejiang Province. Geol. Publ. House, Beijing, p. 617 (in Chinese with English
745 abstract), 1989.

Table 1 Chemical and carbon isotopic compositions of river waters in the Southeast Coastal Rivers Basin (SECRB) of China.

Rivers	Sample number	Date (M/D/Y)	pH	T ℃	EC μs cm^{-1}	Na^+ μM	K^+ μM	Mg^{2+} μM	Ca^{2+} μM	F^- μM	Cl^- μM	NO_3^- μM	SO_4^{2-} μM	HCO_3^- μM	SiO_2 μM	TZ^+ μEq	TZ^- μEq	NICB %	$\delta^{13}C$ ‰	TDS mg l^{-1}
Qiantang*	1	07-8-10	7.42	28.78	190	347	197	106	473	12.0	303	62.6	147	1130	148	1703	1789	-5.0	-19.0	144
	2	07-9-10	7.60	23.84	146	87.5	204	80.9	496	11.7	75.2	124	121	907	156	1446	1348	6.7	-19.8	119
	3	07-9-10	7.37	27.83	308	555	233	208	698	41.8	312	223	437	1170	170	2601	2579	0.9	-17.8	204
	4	07-10-10	7.27	26.28	177	176	135	116	544	15.7	151	142	170	985	175	1632	1618	0.8	-19.3	135
	5	07-10-10	7.05	24.15	123	130	101	66.2	349	17.7	94.3	124	157	529	169	1061	1061	0.0	-18.7	91.2
	6	07-10-10	7.24	23.75	140	97.6	69.7	81.0	451	20.0	62.1	109	204	703	164	1231	1282	-4.2	-21.3	106.6
	7	07-11-10	7.40	23.23	107	92.5	70.5	68.3	327	14.9	74.9	104	147	486	156	954	960	-0.6	-21.0	82.2
	8	07-11-10	7.16	27.61	281	361	87.5	128	469	26.8	245	191	239	810	179	1642	1724	-5.0	-12.9	137.5
	9	07-11-10	7.02	26.48	140	275	120	60.7	319	36.2	199	150	180	437	236	1155	1146	0.8	-13.9	100.2
	10	07-12-10	7.05	24.24	99	205	114	58.3	285	14.6	191	114	132	305	278	1005	874	13.1	-20.9	85.4
	11	07-12-10	7.05	27.01	102	123	133	49.8	284	18.6	86.5	123	144	377	183	924	874	5.4	-19.2	79.4
	12	07-12-10	7.99	24.18	260	50.0	85.4	212	993	-	66.8	153	235	1822	172	2546	2512	1.4	-17.6	205.2
	13	07-12-10	7.86	24.59	231	43.5	88.4	189	859	-	55.1	97.6	169	1763	170	2228	2253	-1.1	-18.7	185.4
	14	07-12-10	7.69	22.66	131	44.1	81.0	113	458	-	19.1	95.2	107	920	143	1266	1248	1.4	-18.1	106.8
	15	07-12-10	7.65	24.48	106	61.1	98.3	87.9	335	-	37.2	68.3	112	663	164	1005	992	1.4	-18.6	87.3
	16	07-12-10	7.46	23.68	125	64.3	108	117	406	-	25.9	75.0	174	687	164	1218	1136	6.7	-20.0	98.8
	17	07-13-10	7.33	24.08	139	59.8	116	136	429	-	29.6	80.4	209	752	162	1305	1281	1.9	-20.8	108.1
	18	07-10-10	7.27	25.74	141	163	114	69.6	396	27.3	126	148	161	597	153	1209	1195	1.1	-21.0	101.0
Cao'e	19	07-16-10	7.17	22.27	108	212	86.3	69.4	183	5.1	151	148	114	384	216	803	912	-13.5	-21.2	79.1
	20	07-16-10	7.06	26.57	182	401	77.6	145	275	18.3	269	185	245	534	215	1318	1478	-12.2	-20.5	116.9
	21	07-16-10	7.14	27.26	171	333	91.3	164	362	18.1	224	194	207	658	225	1475	1490	-1.0	-20.9	123.3
	22	07-16-10	7.08	27.17	173	346	94.4	168	364	18.8	247	200	211	656	222	1506	1526	-1.3	-13.0	125.2
Ling	23	07-15-10	7.07	24.14	52	164	42.9	34.9	140	4.9	40.7	61.5	68.3	277	190	558	516	7.6	-12.8	52.1
	24	07-15-10	7.02	26.04	74	169	92.0	34.2	150	6.4	87.0	77.3	92.8	272	196	629	622	1.1	-20.8	59.5
	25	07-16-10	7.34	25.03	92	159	80.1	47.3	235	19.3	78.0	71.4	105	455	187	804	815	-1.4	-22.5	73.9
	26	07-16-10	7.40	26.75	113	216	77.8	57.1	249	20.2	133	90.0	115	494	196	905	946	-4.5	-12.7	82.8
	27	07-16-10	7.39	26	89	174	86.4	56.4	209	9.0	99.3	78.4	99.9	420	199	792	798	-0.8	-14.0	72.7
	28	07-15-10	6.79	22.33	75	159	82.7	44.1	143	-	107	61.8	83.4	306	144	616	641	-4.1	-21.1	56.5
	29	07-15-10	8.24	27.15	129	228	92.1	83.1	317	17.2	177	90.5	120	641	194	1120	1148	-2.5	-19.2	97.8
Ou	30	07-13-10	8.08	28.45	48	95.2	107	38.4	92.1	15.2	31.8	43.3	47.4	291	221	463	461	0.4	-21.7	50.6
	31	07-13-10	6.71	22.97	32	60.7	106	12.6	65.0	10.8	28.9	45.0	48.9	158	169	322	329	-2.2	-23.8	36.9
	32	07-13-10	7.18	27.59	73	107	127	36.2	175	4.3	57.1	111	92.0	283	210	655	634	3.2	-23.4	62.9
	33	07-13-10	6.94	24.2	44	76.9	112	20.0	99.1	10.9	27.9	63.1	58.6	249	184	427	457	-7.0	-22.5	47.5
	34	07-14-10	7.16	27.45	90	187	127	41.2	199.5	17.0	85.6	102	116	367	251	796	787	1.1	-22.4	76.5
	35	07-14-10	6.97	24.56	54	105	50.9	29.2	122	12.2	46.1	67.8	73.1	218	193	460	478	-4.1	-22.5	47.9
	36	07-14-10	6.82	21.12	31	76.4	133	12.7	74.5	7.7	20.7	36.8	49.1	192	162	383	348	9.3	-	39.5
	37	07-14-10	6.82	23.69	45	89.5	105	19.0	97.8	10.6	39.6	52.8	59.1	231	185	428	441	-3.0	-22.9	46.2
	38	07-15-10	6.92	24.69	37	100	89.3	21.1	49.7	1.7	36.9	45.5	52.7	153	202	331	341	-2.9	-	38.9
	39	07-15-10	6.90	23.86	35	92.2	92.0	19.8	61.4	1.9	43.9	47.9	55.5	139	193	347	342	1.4	-22.3	38.5
	40	07-15-10	7.09	25.56	47	117	112	25.7	83.4	8.0	52.4	63.1	57.4	232	193	447	462	-3.3	-22.5	48.1
	41	07-14-10	6.97	24.25	53	102	107	27.6	119	13.4	43.5	59.4	73.2	277	183	502	526	-4.9	-13.7	52.3

Feiyun	42	07-17-10	7.28	25.19	38	94.0	81.7	24.0	75.6	11.4	59.9	45.7	51.9	149	151	375	358	4.5	-	37.2
	43	07-17-10	7.08	25.61	46	101	79.9	33.9	93.4	4.6	66.2	55.1	52.8	223	151	435	450	-3.3	-23.7	43.5
Jiaoxi	44	07-17-10	7.52	26.92	47	116	81.5	25.2	92.0	4.1	73.3	80.3	25.0	226	151	432	430	0.5	-23.4	43.0
	45	07-17-10	7.45	27.46	61	152	90.2	34.2	119	-	136	59.8	53.5	238	184	548	542	1.2	-23.1	51.8
	46	07-18-10	6.90	27.66	53	127	88.1	33.4	94.4	7.0	123	93.1	30.4	209	177	471	486	-3.3	-14.4	47.4
Huotong	47	07-18-10	7.34	24	43	116	78.8	26.1	58.4	5.4	68.7	49.7	20.1	197	190	364	355	2.3	-22.8	39.6
Ao	48	07-19-10	7.24	31.44	124	294	121	102	209	24.3	204	73.6	52.0	717	370	1036	1100	-6.1	-19.4	105.4
	49	07-19-10	7.13	27.82	46	109	96.3	30.0	73.8	-	72.0	51.3	22.5	234	236	413	402	2.6	-	46.2
	50	07-18-10	6.98	28.65	53	140	88.4	40.8	100	3.0	82.9	58.6	20.9	294	233	511	477	6.6	-22.3	52.2
Min	51	07-27-10	7.11	28.4	42	116	92.0	40.5	119	18.0	43.9	35.5	26.0	382	182	526	513	2.4	-19.4	52.7
	52	07-27-10	7.17	30	51	102	97.9	41.7	107	4.6	29.4	45.3	35.0	350	221	496	495	0.2	-	53.3
	53	07-27-10	7.08	29.4	99	214	92.7	46.4	126	18.4	50.1	39.8	118	327	154	651	654	-0.4	-20.8	74.0
	54	07-27-10	7.06	29.1	44	107	99.6	28.1	114	16.4	18.7	36.4	44.3	305	265	491	449	8.5	-17.6	53.6
	55	07-27-10	7.42	29.4	57	139	93.7	49.8	113	3.1	67.1	56.3	26.6	384	236	558	561	-0.5	-16.4	58.6
	56	07-27-10	7.12	27.8	51	103	91.0	50.8	106	4.7	82.8	35.1	63.5	249	225	507	494	2.5	-	51.3
	57	07-27-10	7.08	27.5	40	125	45.0	36.8	107	12.1	43.6	44.5	29.3	288	211	457	435	5.0	-21.1	47.4
	58	07-27-10	6.99	27.2	52	121	98.0	42.4	115	16.7	87.1	36.6	70.9	277	228	535	542	-1.4	-11.4	55.3
	59	07-27-10	6.87	29	59	154	91.4	59.4	124	16.5	77.8	36.7	88.3	272	222	612	563	8.0	-20.3	57.2
	60	07-27-10	7.31	27.1	78	109	92.1	59.1	181	21.2	123	37.5	78.4	355	202	682	672	1.4	-18.7	63.1
	61	07-27-10	7.22	27.8	37	122	83.3	52.8	142	17.4	111	37.3	80.4	288	221	596	597	-0.2	-22.3	58.1
	62	07-27-10	7.16	28.1	58	104	83.3	59.3	163	24.0	34.6	34.5	118	294	214	632	599	5.2	-13.4	59.5
	63	07-27-10	7.26	28.3	87	139	86.1	60.9	191	14.8	48.0	93.0	109	347	226	729	707	3.0	-21.4	68.6
	64	07-27-10	7.00	28.8	87	127	93.1	58.7	195	6.6	59.8	81.1	60.9	480	232	729	743	-2.0	-11.0	74.0
	65	07-28-10	6.97	27.9	37	163	82.1	52.2	140	20.2	53.1	60.0	106	306	221	630	632	-0.2	-	61.9
	66	07-13-10	7.07	27.96	59	91.9	110	40.0	127	24.8	62.0	79.3	62.3	249	228	535	515	3.8	-	54.8
	67	07-28-10	7.12	29.7	38	108	93.4	45.9	133	12.4	48.3	34.0	56.6	368	220	560	564	-0.7	-	57.7
	68	07-27-10	7.03	29.9	62	128	96.7	57.6	148	23.3	81.6	36.8	74.1	374	203	635	641	-0.9	-12.4	61.7
	69	07-27-10	7.01	28.8	60	102	89.1	73.6	138	9.6	50.6	74.1	32.7	417	233	615	607	1.3	-21.0	62.3
	70	07-27-10	7.06	26.5	37	93.5	93.1	34.7	87.3	-	26.6	34.8	37.1	312	222	431	448	-3.9	-13.1	49.1
	71	07-27-10	7.09	26.5	25	62.6	92.7	27.0	61.5	4.7	21.5	18.6	43.4	191	154	332	318	4.2	-16.0	35.3
	72	07-28-10	7.07	30.1	39	76.3	87.9	35.1	87.6	7.4	43.1	36.6	35.5	266	175	409	416	-1.7	-19.4	43.5
	73	07-27-10	7.01	28.7	47	84.9	95.4	56.7	106	12.7	51.8	49.2	57.2	315	211	506	531	-4.8	-	53.8
	74	07-27-10	6.85	28.7	50	93.6	85.9	52.4	107	14.1	62.8	57.5	57.0	252	217	498	487	2.2	-19.9	50.9
	75	07-27-10	7.11	29.7	69	117	85.2	73.4	159	7.6	63.7	75.2	47.4	418	230	666	652	2.2	-22.2	65.0
	76	07-28-10	6.93	28.9	59	112	88.0	61.8	122	6.0	57.4	89.3	42.0	349	224	568	580	-2.2	-22.0	58.8
	77	07-21-10	7.76	32.4	51.2	163	85.5	52.8	151	20.2	55.3	70.3	78.6	372	175	656	655	0.3	-12.5	61.8
	78	07-28-10	7.29	26.8	106	129	75.3	84.0	321	24.0	56.2	41.0	166	599	202	1013	1028	-1.4	-16.3	90.3
	79	07-21-10	7.09	26.96	56	112	87.6	37.1	129	4.5	51.5	44.9	61.9	327	276	531	547	-2.9	-22.2	59.1
	80	07-21-10	7.64	33.37	83	114	96.2	60.6	151	16.7	53.0	40.6	102	371	242	633	670	-5.8	-12.8	66.2
	81	07-21-10	7.83	31.27	65	131	102	52.7	141	16.1	45.3	49.7	91.8	324	239	620	603	2.8	-13.4	61.8
	82	07-21-10	6.84	28.35	66	132	101	52.5	141	5.8	63.8	54.1	91.6	304	243	621	606	2.5	-22.7	61.5
	83	07-21-10	7.42	30.7	98	217	113	59.2	210	18.4	98.7	63.5	84.7	496	320	868	827	4.6	-18.9	84.5
	84	07-27-10	7.26	26.3	46	104	102	29.7	121	3.6	55.2	51.9	55.5	294	193	507	512	-0.9	-21.6	51.9
	85	07-27-10	7.07	25.4	30	73.3	99.2	19.6	78.8	-	22.9	40.0	49.2	203	170	369	365	1.3	-21.1	39.8
	86	07-27-10	7.50	27.3	45	102	102	26.5	114	2.4	35.1	39.7	57.2	260	217	484	449	7.3	-15.7	49.6
	87	07-27-10	7.47	26.9	51	141	100	43.6	109	7.9	79.7	42.4	57.7	311	217	547	548	-0.3	-20.1	55.6

	88	07-19-10	7.99	31.74	63	167	96.5	33.5	115	8.0	105	35.5	38.1	331	218	561	548	2.3	-13.5	55.9
	89	07-21-10	6.77	28.19	65	132	93.6	56.0	145	15.6	60.6	78.8	75.4	333	243	627	624	0.5	-22.6	63.3
Jin	90	07-27-10	7.36	25.8	128	126	94.8	88.9	406	22.9	51.4	39.4	229	595	208	1211	1143	5.6	-20.7	100
	91	07-27-10	7.40	26.9	123	143	103	82.7	347	21.0	83.5	203	182	463	226	1105	1115	-0.9	-21.3	98.4
	92	07-27-10	7.00	27.4	88	170	98.8	56.8	205	7.2	137	117	106	327	205	793	792	0.1	-22.5	71.8
	93	07-27-10	7.32	28.7	73	201	116	87.1	318	20.0	93.5	41.5	189	508	267	1128	1020	9.6	-21.7	95.3
Jiulong	94	07-30-10	6.50	23.47	29	72.3	92.4	22.8	59.8	12.4	25.1	27.0	50.0	189	213	330	341	-3.4	-18.1	40.1
	95	07-30-10	7.06	29.35	120	136	96.9	106	339	5.1	67.7	66.3	249	469	202	1124	1100	2.1	-20.8	94.2
	96	07-30-10	7.45	27.6	104	79.5	97.5	106	363	14.4	70.7	50.0	99.9	729	184	1116	1049	6.0	-18.9	93.7
	97	07-31-10	7.36	26.59	139	140	100	142	432	15.5	79.6	78.3	274	573	196	1388	1278	8.0	-19.7	108.8
	98	07-31-10	7.72	26.18	88	77.6	96.2	69.0	313	19.9	39.7	34.6	63.8	731	251	938	933	0.5	-18.4	89.4
	99	07-30-10	7.43	26.96	119	200	93.8	100.2	298	19.9	122	80.5	225	387	202	1091	1040	4.7	-20.5	89.5
	100	07-28-10	7.41	26.66	112	173	97.9	94.4	286	46.1	118	152	201	364	207	1033	1036	-0.3	-20.9	92.2
	101	07-29-10	7.16	29.35	82	151	110	55.4	178	4.9	71.2	170	53.2	385	305	727	732	-0.7	-21.2	76.1
	102	07-29-10	7.10	28.9	100	222	98.3	49.4	249	3.6	126	157	52.7	532	303	917	920	-0.3	-21.7	90.0
	103	07-28-10	7.20	31.15	138	339	111	81.2	277	9.2	280	285	88.6	515	317	1165	1256	-7.8	-19.0	112
	104	07-28-10	7.16	27.09	101	261	95.8	81.7	235	40.3	173	80.1	174	291	136	990	892	9.9	-24.3	75.4
Zhang	105	07-28-10	8.08	30.6	93	195	96.1	61.1	167	16.8	157	193	55.2	281	288	748	741	0.9	-21.5	73.8
Dongxi	106	07-28-10	7.20	30.9	78	263	99.0	41.5	115	14.5	238	65.3	30.0	283	309	675	646	4.4	-20.8	66.7
Huangang	107	07-28-10	7.40	30.5	99	253	85.6	53.0	154	7.7	190	63.5	56.4	460	278	754	827	-9.6	-20.0	77.4
Han	108	07-31-10	7.31	27.1	68	136	61.5	45.2	195	16.1	37.7	45.3	93.7	345	218	678	615	9.2	-21.9	62.0
	109	07-30-10	7.38	26.94	88	116	103	63.6	265	6.4	53.4	72.2	84.9	584	244	876	879	-0.4	-20.4	83.7
	110	07-30-10	6.66	25.55	71	114	96.2	47.6	168	8.0	56.9	54.6	143	230	203	642	628	2.2	-17.9	59.7
	111	07-30-10	6.66	27.76	83	135	104	63.8	203	8.6	54.5	74.9	173	302	336	774	777	-0.4	-20.6	78.7
	112	07-30-10	7.31	30.81	56	168	74.0	39.1	118	13.5	62.9	44.4	81.4	237	245	556	507	8.8	-21.4	54.6
	113	07-31-10	7.28	28.73	98	137	99.3	85.6	270	9.2	88.8	59.1	118	565	233	948	949	-0.1	-19.7	86.6
	114	07-31-10	7.27	31.42	123	193	105	98.2	319	20.7	120	102	157	570	229	1132	1107	2.2	-19.7	98.2
	115	07-30-10	7.43	29.89	85	115	97.5	65.5	244	6.5	46.5	58.6	103	511	251	832	822	1.1	-20.8	79.3
	116	07-31-10	7.61	30.98	99	123	104	85.9	264	5.6	58.8	90.9	108	588	98	926	952	-2.9	-20.0	79.4
	117	07-31-10	7.31	29.96	93	151	103	78.1	250	15.4	68.0	99.1	173	379	233	909	891	1.9	-21.9	81.8
	118	07-31-10	7.35	28.4	2	233	84.2	101	323	12.8	84.0	101	203	460	229	1165	1051	9.8	-21.1	94.7
	119	07-31-10	7.67	30.38	93	136	87.8	73.6	231	16.4	64.6	94.4	184	382	226	834	909	-9.1	-20.8	80.5
Rong	120	07-30-10	7.57	31.83	68	193	79.1	50.3	146	16.4	192	84.0	31.5	344	309	664	683	-2.8	-20.3	65.8
	121	07-30-10	6.96	30.62	94	509	103	56.1	213	15.9	511	78.5	82.3	379	222	1150	1133	1.5	-20.0	94.4

TZ^+ is the total cationic charge; TZ^- is the total anionic charge; NICB is the normalized inorganic charge balance and TDS is the total dissolved solid.

*data of major ion composition are from Liu et al. (2016).

Table 2 Chemical compositions of precipitation at different sites located within the studied area (in μmol l^{-1} and molar ratio).

Province	Location	pH	F^-	Cl^-	NO_3^-	SO_4^{2-}	NH_4^+	K^+	Na^+	Ca^{2+}	Mg^{2+}	NO_3/Cl	SO_4/Cl	K/Cl	Na/Cl	Ca/Cl	Mg/Cl	Reference
Zhejiang	Hangzhou	4.5	5.76	13.9	38.4	55	79.9	4.18	12.2	26	3.53	2.76	3.96	0.3	0.88	1.87	0.25	Xu et al., 2011
	Jinhua	4.54	9.05	8.51	31.2	47.6	81.1	4.73	6.27	24	1.73	3.67	5.59	0.56	0.74	2.81	0.2	Zhang et al., 2007
Fujian	Nanping	4.81	0.8	5.8	26.6	18.3	38	4.9	5.4	12.9	2.7	4.59	3.16	0.84	0.93	2.22	0.47	Cheng et al., 2011
	Fuzhou		5.26	21.4	24.9	48.5	78.1	4.1	2.61	32.7	1.25	1.16	2.26	0.19	0.12	1.53	0.06	Zhao, 2004
	Xiamen	4.57	15.3	23.7	22.1	31.3	37.7	3.58	36.1	21.5	4.94	0.93	1.32	0.15	1.52	0.91	0.21	Zhao, 2004
Average												2.62	3.26	0.41	0.84	1.87	0.24	

Table 3 Contribution of each reservoir, fluxes, chemical weathering and associated CO_2 consumption rates for the major rivers and their main tributaries in the SECRB.

Major river	Tributaries	Location	Discharge	Area	Runoff	Contribution (%)				Fluxes (10^6 t a^{-1})		Weathering rate (t $km^{-2}a^{-1}$)				CO_2 consumption rate (10^3 mol km^{-2} a^{-1})			
			10^9 m^3a^{-1}	10^3 km^2	mm a^{-1}	Rain	Anth.	Sil.	Carb.	SWF	CWF	Cat_{sil}[a]	SWR[b]	CWR[b]	TWR[b]	CSW[c]	CCW[c]	SSW[d]	$SNSW$[e]
Qiantang		Fuyang	43.81	38.32	1143	9	14	23	54	0.66	1.74	6.8	17.3	45.3	62.6	223	459	195	184
	Fenshui	Tonglu	2.726	3.100	879	7	14	18	62	0.05	0.16	5.5	14.7	52.1	66.8	167	530	152	146
Cao'e		Huashan	2.610	3.043	858	7	23	26	44	0.06	0.11	6.8	18.2	35.4	53.5	269	369	240	229
Ling		Linhai	5.400	6.613	817	9	22	24	45	0.09	0.17	4.7	14.2	26.1	40.3	167	267	143	133
	Yonganxi	Baizhiao	3.184	2.475	1286	14	15	50	21	0.06	0.03	9.1	24.2	11.7	35.9	350	119	255	216
	Shifengxi	Shaduan	1.731	1.482	1168	11	19	35	36	0.03	0.04	7.6	21.4	24.5	45.9	304	249	249	227
Ou		Hecheng	20.65	13.45	1536	20	6	56	18	0.36	0.13	10.1	26.9	9.9	36.9	360	101	228	174
	Haoxi	Huangdu	1.809	1.270	1447	16	8	46	30	0.04	0.02	9.9	27.9	19.0	46.9	336	192	246	210
	Xiaoxi	Jupu	5.116	3.336	1534	23	0	74	4	0.09	0.01	11.4	26.4	1.8	28.2	391	18	202	125
	Nanxi	Yongjiashi	1.799	1.273	1413	21	9	63	7	0.03	0.00	10.0	26.3	3.3	29.6	360	34	200	135
Huotong		Yangzhong	3.470	2.082	1667	22	18	54	5	0.06	0.00	8.3	27.3	2.1	29.4	305	24	129	59
Ao		Lianjiang	2.770	3.170	874	17	17	48	17	0.05	0.02	5.1	17.3	5.4	22.7	188	56	122	95
Min		Zhuqi	84.59	54.50	1552	15	10	48	27	1.80	0.94	10.3	33.0	17.3	50.2	390	180	292	252
	Futun	Yangkou	22.53	12.67	1778	15	14	49	22	0.45	0.21	12.0	35.8	16.2	52.0	460	171	336	286
	Shaxi	Shaxian	12.87	9.922	1297	13	9	42	36	0.26	0.21	8.4	26.5	21.7	48.1	315	222	249	223
	Jianxi	Qilijie	24.91	14.79	1685	16	10	45	29	0.48	0.26	9.6	32.2	17.4	49.6	350	185	250	210
	Youxi	Youxi	5.237	4.450	1177	15	8	46	31	0.11	0.07	7.4	24.5	15.0	39.5	272	156	205	178
	Dazhangxi	Yongtai	4.205	4.034	1042	15	21	47	17	0.08	0.03	6.6	20.2	7.1	27.4	242	73	163	131
Jin	Xixi	Anxi	3.004	2.466	1218	9	10	29	52	0.06	0.10	7.9	24.4	42.2	66.6	284	430	247	232
	Dongxi	Honglai	2.236	1.704	1312	12	22	28	38	0.04	0.04	6.8	22.9	25.6	48.5	226	263	178	158
Jiulong		Punan	10.20	8.49	1201	13	14	28	45	0.19	0.29	7.3	22.2	34.0	56.2	263	351	209	188
	Xi'xi	zhengdian	4.080	3.420	1193	10	32	25	33	0.10	0.11	8.0	30.7	30.9	61.6	288	317	227	203
Zhang		Yunxiao	1.011	1.038	974	16	25	29	29	0.02	0.01	5.1	21.9	14.1	36.0	174	146	114	90
Dongxi		Zhao'an	1.176	0.955	1231	16	41	26	17	0.03	0.01	5.8	28.7	10.2	38.9	187	107	93	55
Huanggang		Raoping	1.637	1.621	1010	15	30	34	21	0.04	0.02	6.0	22.8	11.1	33.9	227	115	145	112
Han		Chao'an	24.75	29.08	851	16	7	38	39	0.49	0.50	5.4	17.0	17.0	34.0	208	176	156	135

Ding	Xikou	11.14	9.228	1207	17	6	46	32	0.31	0.18	9.0	33.3	19.1	52.4	341	196	249	212
Mei	Hengshan	10.29	12.95	794	12	13	31	44	0.21	0.32	5.7	16.6	24.5	41.1	212	252	173	157
Whole SECRB		207	167	1240					3.95	4.09	7.8	23.7	24.5	48.1	287	251	218	191

[a] Cat_{sil} are calculated based on the sum of cations from silicate weathering.

[b] SWR, CWR and TWR represent silicate weathering rates (assuming all dissolved silica is derived from silicate weathering), carbonate weathering rates and total weathering rates, respectively.

[c] CO_2 consumption rate with assumption that all the protons involved in the weathering reaction are provided by carbonic acid.

[d] Estimated CO_2 consumption rate by silicate weathering when H_2SO_4 from acid precipitation was taken into account.

[e] Estimated CO_2 consumption rate by silicate weathering when both H_2SO_4 and HNO_3 from acid precipitation were taken into account.

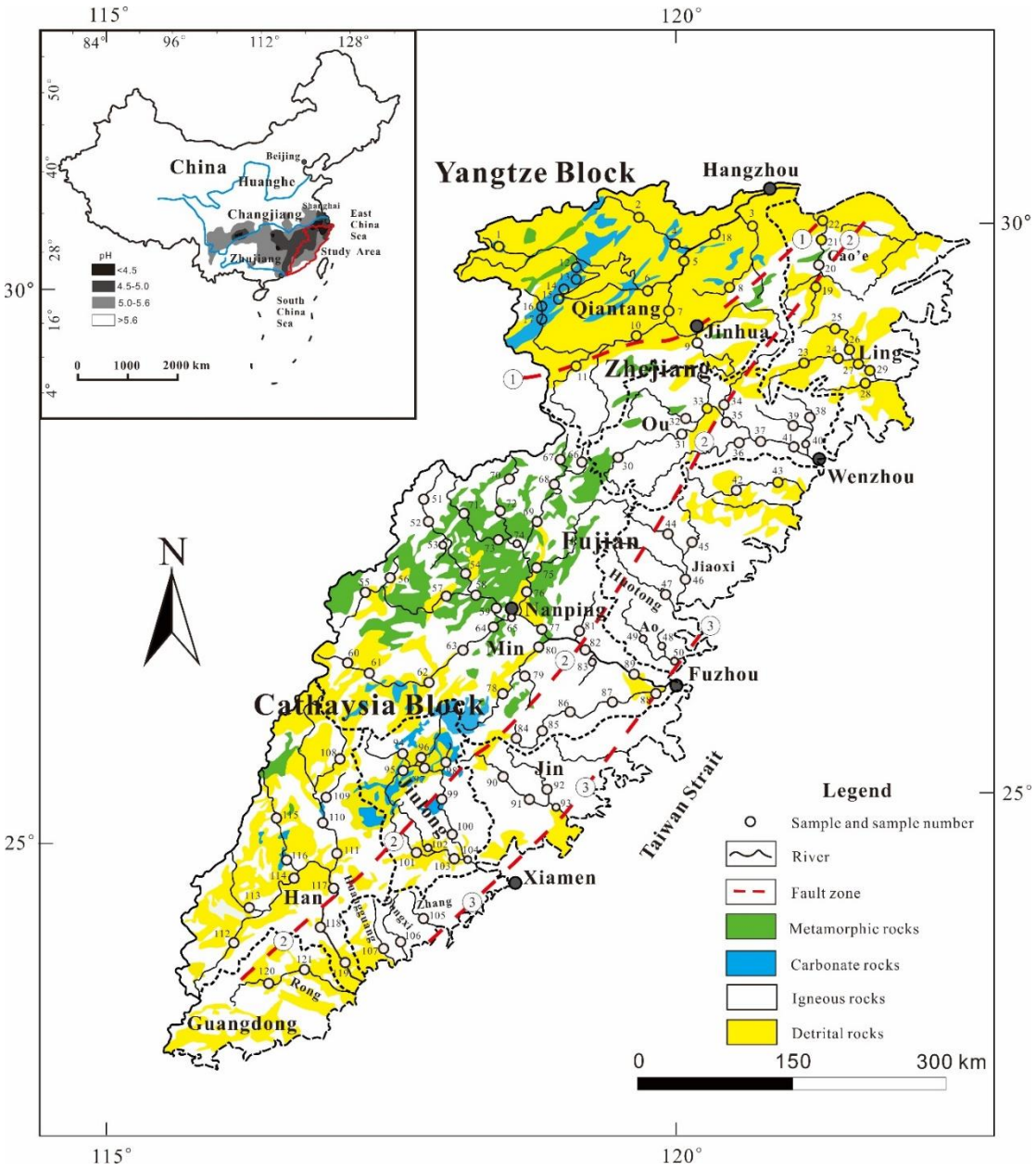

Fig. 1. Sketch map showing the lithology, sampling locations, and sample number of the SECRs drainage basin, and regional rain water pH ranges are shown in the sketch map at the upper-left. (modified from Zhou and Li, 2000; Shu et al., 2009; Xu et al., 2016, rain water acidity distribution of China mainland is from State Environmental Protection Administration of China). ①Shaoxing-Jiangshan fault zone; ②Zhenghe-Dapu fault zone; ③Changle-Nanao fault zone. The figure was created by CorelDraw software version 17.1.

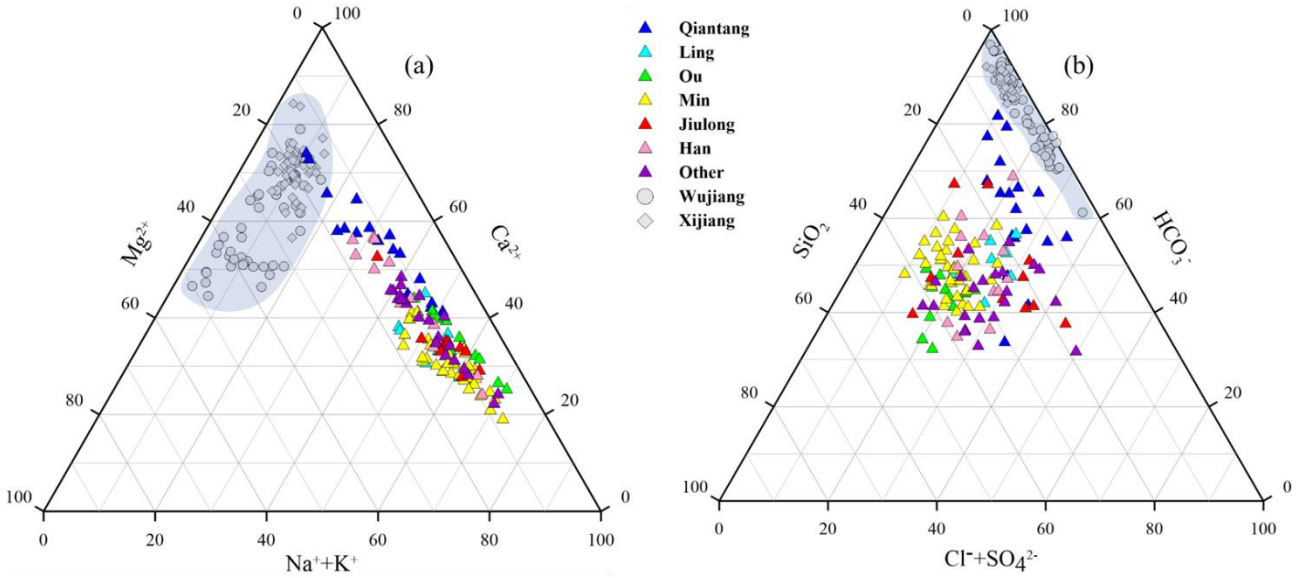

Fig. 2. Ternary diagrams showing cations (a), anions and dissolved SiO_2 (b) compositions of river waters in the SECRB. Chemical compositions from case studies of rivers draining carbonate rocks (the Wujiang and the Xijiang) are also shown for comparison (data from Han and Liu 2004; Xu and Liu 2007, 2010).

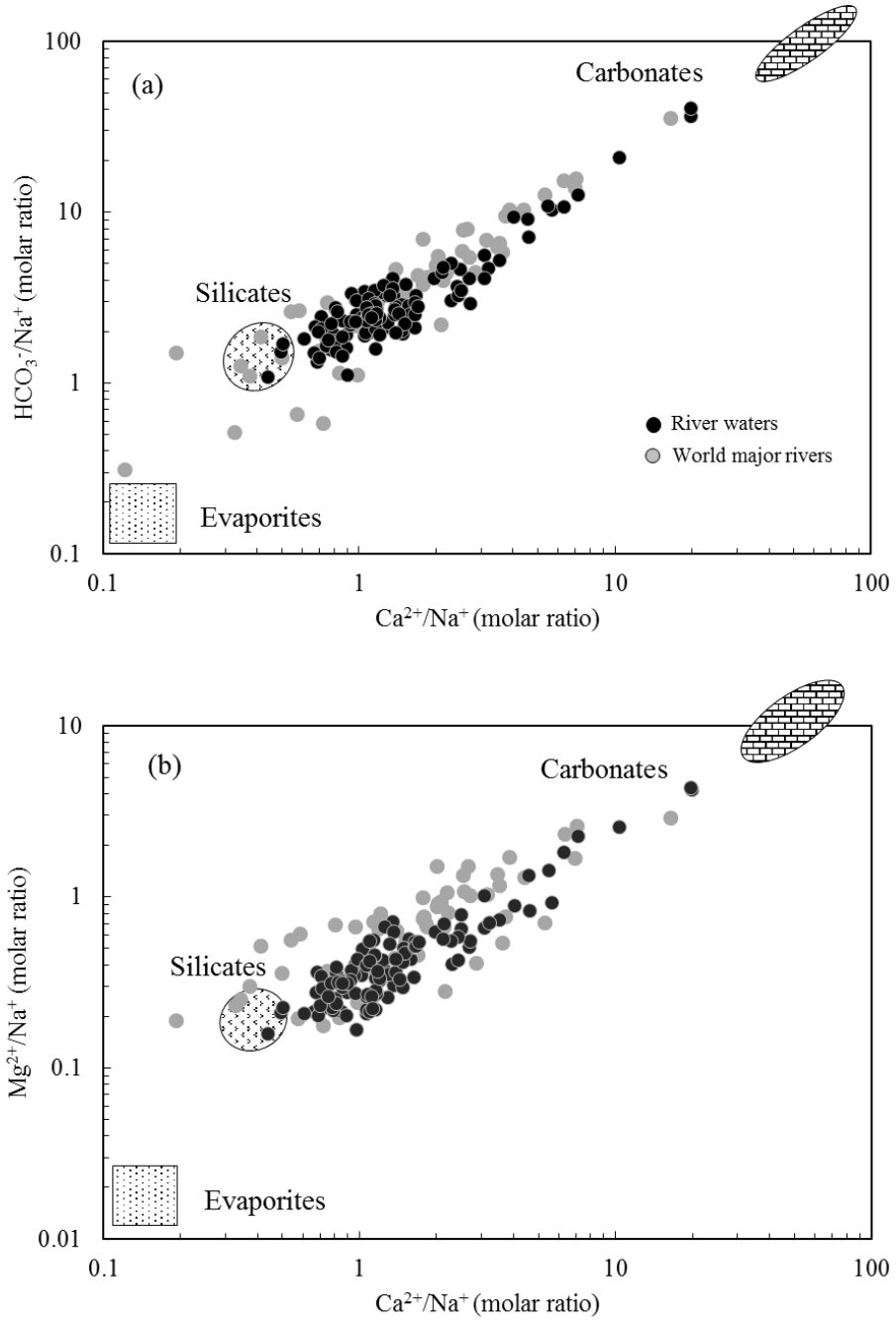

Fig. 3. Mixing diagrams using Na-normalized molar ratios: HCO_3^-/Na^+ *vs.* Ca^{2+}/Na^+ (a) and Mg^{2+}/Na^+ *vs.* Ca^{2+}/Na^+ (b) for the SECRB. The samples mainly cluster on a mixing line between silicate and carbonate end-members. Data for world major rivers are also plotted (data from Gaillardet et al. 1999).

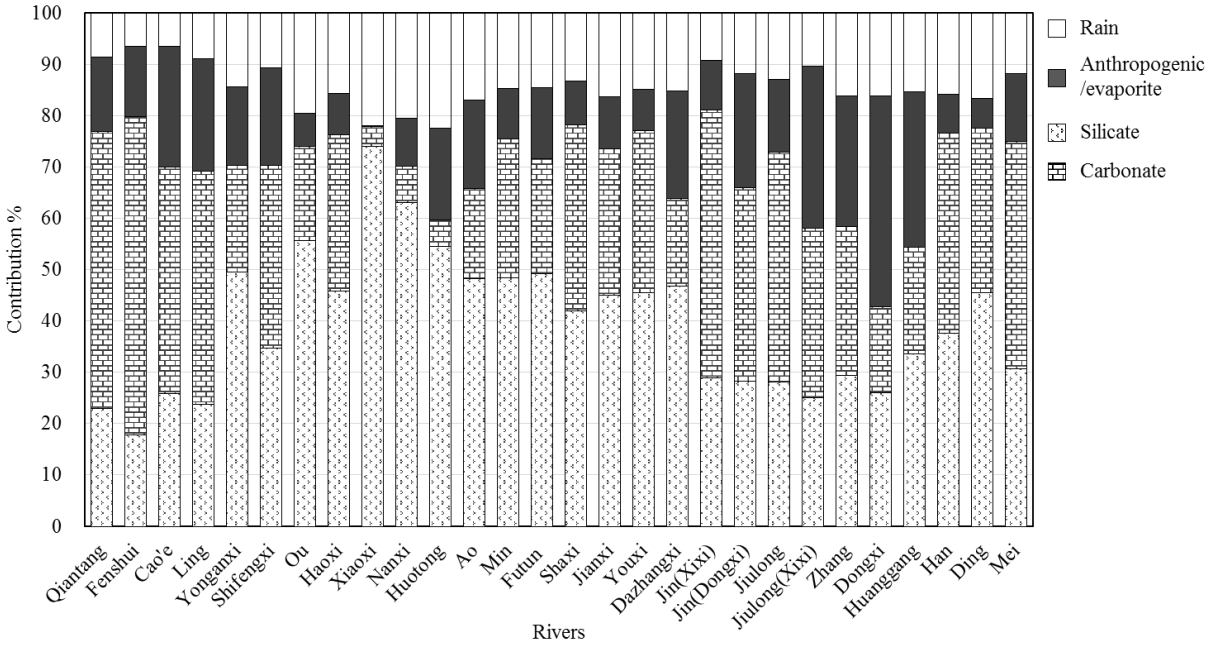

Fig. 4. Calculated contributions (in %) from the different reservoirs to the total cationic load for major rivers and their main tributaries in the SECRB. The cationic loads are the sum of Na^+, K^+, Ca^{2+} and Mg^{2+} from different reservoirs.

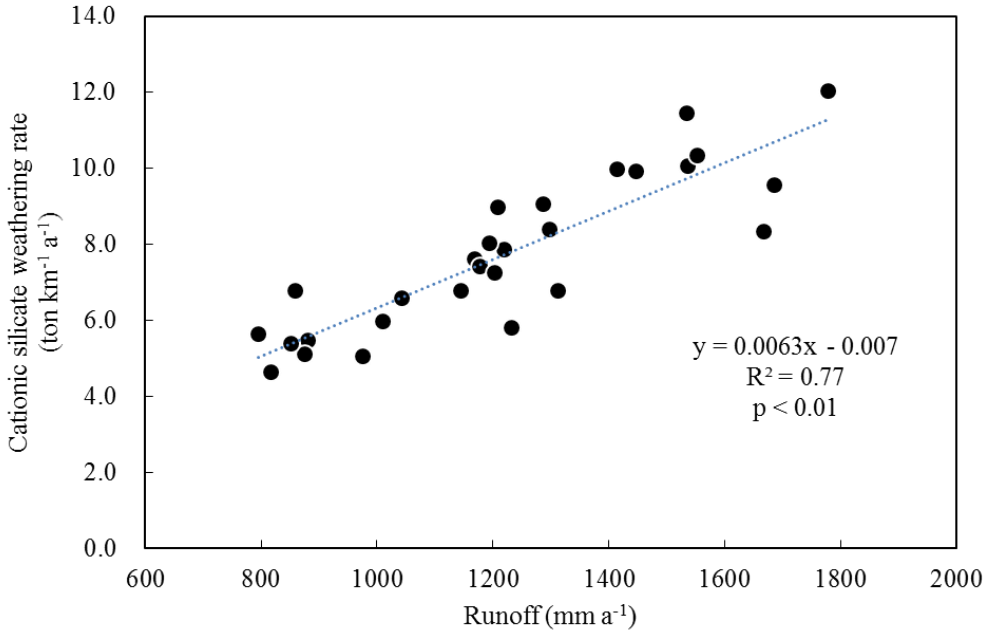

Fig. 5. Plots of the cationic-silicate weathering rate (Cat_{sil}) vs. runoff for the SECRB.

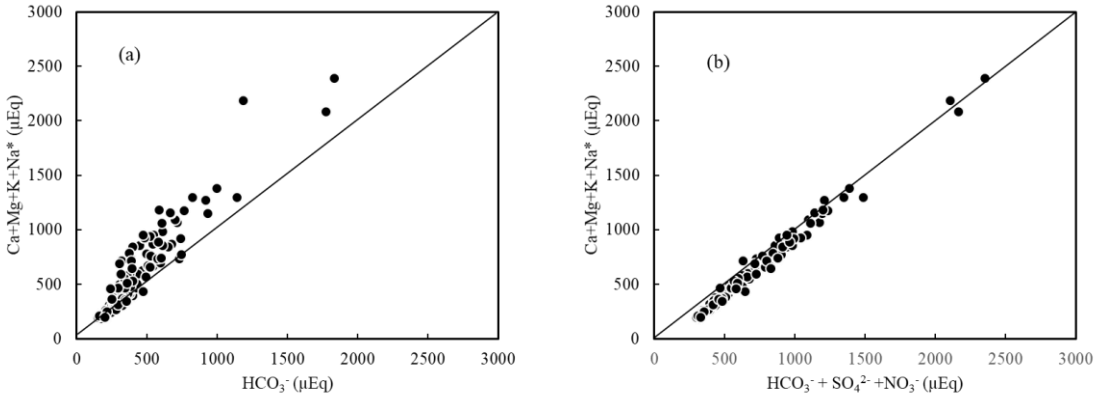

Fig. 6. Plots of total cations derived from carbonate and silicate weathering *vs.* HCO_3^- (a) and $HCO_3^-+SO_4^{2-}+NO_3^-$ (b) for river waters in the SECRB.

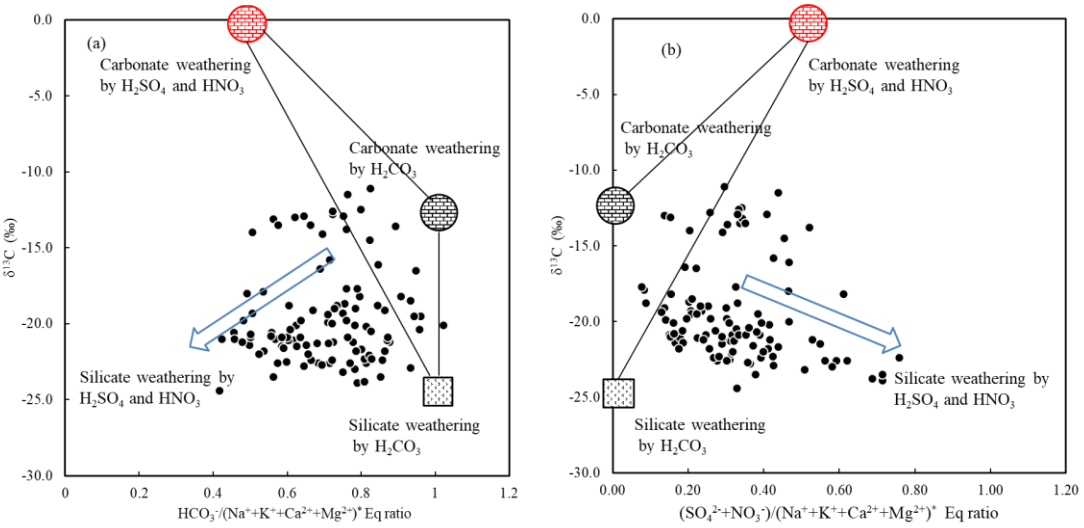

Fig. 7. $\delta^{13}C_{DIC}$ *vs.* $HCO_3^-/(Na^++K^++Ca^{2+}+Mg^{2+})^*$ (a) and $(SO_4^{2-}+NO_3^-)/(Na^++K^++Ca^{2+}+Mg^{2+})^*$ equivalent ratio (b) in river waters draining the SECRB (* noted concentrations corrected for atmospheric and anthropogenic inputs). The plots show that most waters deviate from the three end-member mixing area (carbonate weathering by carbonic acid and sulfuric/nitric acid and silicate weathering by carbonic acid).